UNIVERSITY of LIMERICK

OLLSCOIL LUIMNIGH

Crystallisation Thermodynamics

Masood Valavi

Supervisor: Professor Åke C. Rasmuson

Master's thesis submitted to the Faculty of Science and Engineering, University of Limerick, Limerick

Ireland, 2016

Declaration

I declare that the contents of this thesis, except where reference is made, are my original work and that it has not been previously submitted to any university for a degree.

Masood Valavi

Acknowledgments

I would like to express my gratitude to Professor Rasmuson for being so generous with his time and for his continuous valuable advice.

Grateful thanks as well to members of the SSPC for their help and fruitful discussions.

I also would like to thank my family for their support.

List of publications

1- "Thermodynamic Stability Analysis of Tolbutamide Polymorphs and Solubility in Organic Solvents" Michael Svärd, **Masood Valavi,** Dikshitkumar Khamar, Manuel Kuhs and Åke Rasmuson. **Published in the Journal of Pharmaceutical Sciences**

2-"Prediction of the Solubility of Medium-Sized Pharmaceutical Compounds using a Temperature-Dependent NRTL-SAC Model" **Masood Valavi,** Michael Svärd and Åke Rasmuson. **Published in the Journal of Industrial and Engineering Chemistry Research**

3-"Improving Estimates of the Crystallization Driving Force: Investigation into the Dependence on Temperature and Composition of Activity Coefficients in Solution" **Masood Valavi,** Michael Svärd and Åke Rasmuson. **Published in the Journal of Crystal Growth and Design.**

4-"Thermodynamics of Butamben" **Masood Valavi,** Michael Svärd and Åke Rasmuson, **In preparation**

Table of Contents

Abstract

This study investigated two important thermodynamic parameters of crystallisation: the activity coefficient and solubility. The influence of composition and temperature on the activity coefficient was investigated to provide a better approximation of the driving force of crystallisation. It was found that the influence of temperature on the activity coefficient was generally much smaller than the influence of composition. Based on an analysis that was performed, a new estimation of the driving force was suggested. Since the driving force is also dependent on solubility, it is important to have an accurate estimation of solubility. Three models were used to calculate a solubility curve: “original NRTL-SAC”, “temperature-dependent NRTL-SAC” and “Pharma UNIFAC”. A comparison between the performances of these three models was presented. It was found that introducing a temperature-dependent binary interaction parameter to the original NRTL-SAC model could improve this model’s performance in calculating solubility. However, as the experimental determination of solubility has a huge influence on the yield of harvested crystals, the solubilities of two APIs – tolbutamide and butamben – were measured experimentally. The solubility of both APIs increased with increasing temperature in all solvents. The thermodynamics of the compound butamben in solution was also investigated in this project.

Symbols

μ^{solid}	Chemical potential of solid
μ^{solute}	Chemical potential of solute
μ^{l}	Chemical potential of supercooled melt
γ^{sat}	Saturated activity coefficient
x^{sat}	Solubility (mole fraction)
$\Delta G^{fus}(T)$	Gibbs free energy of fusion at T
$\Delta H^{fus}(T)$	Enthalpy of fusion at T
$\Delta H^{fus}(T)$	Entropy of fusion at T
T	Temperature
T_m	Melting temperature
ΔC_p	Difference between heat capacity of supercooled melt and solid
C_p^l	Heat capacity of supercooled melt
C_p^s	Heat capacity of solid
$\Delta\mu$	Driving force of crystallisation
τ_{ij}	Binary interaction parameter in NRTL-SAC model
α_{ij}	Non-randomness NRTL parameter in NRTL-SAC model
R_k	Pharma UNIFAC parameter
Q_k	Pharma UNIFAC parameter
ΔH^{vH}	van't Hoff enthalpy of solution
A_{12}	Van Laar binary interaction parameter
ΔH^{mix}	Mixing enthalpy
x_1	Molar concentration at point 1
x_3	Molar concentration at point 3

Chapter 1: Introduction and theory

Crystallisation is a process that is used in the production of salts, active pharmaceutical ingredients (API) *etc*. About 90 % of pharmaceutical products contain crystalline material [1], making the crystallisation process hugely important in the pharmaceutical industry. There are two parts to this process: nucleation and crystal growth. Nucleation and growth processes continue for as long as there is a driving force for crystallisation. The driving force of the crystallisation depends on supersaturation and the activity coefficient ratio (ratio of the activity coefficient in supersaturation to the activity coefficient at equilibrium). Hence the rates of nucleation and growth also depend on supersaturation and the activity coefficient ratio. Based on crystallisation conditions, either nucleation or growth may dominate over the other, and as a result crystals will have different sizes and shapes [2].

Furthermore, many compounds have the ability to crystallise with different crystal structures. This phenomenon is called polymorphism. Each polymorph has a different thermodynamic solid state. Crystal polymorphs of the same compound may exhibit different physical properties, such as dissolution rate, shape, melting point *etc*.[2] For this reason, polymorphism is hugely important in the industrial manufacture of crystalline products. Depending on the crystallisation conditions (*e.g.* temperature and cooling rate), control over polymorphism can be achieved.

Both thermodynamics and kinetics play important roles in crystallisation. Thermodynamics influences the driving force and the control of polymorphism during crystallisation and therefore control over the thermodynamics of the process is important in order to produce crystals of the desired shape and size.

There are two parameters that play significant roles in the thermodynamics of crystallisation: solubility and the activity coefficient. Solubility of the API affects the bioavailability of the drug, but also controls supersaturation and particle size and yield during crystallisation. The activity coefficient and its magnitude along the solubility curve, as well as in conditions of supersaturation, can greatly influence the estimation of the driving force for crystallisation and in turn the thermodynamics of crystallisation.

Solubility can be determined experimentally, but this is often time-consuming and expensive. Alternatively, solubility can be predicted using activity coefficient models. There are many studies focusing on the theoretical calculation of solubility using models. These models are divided into three groups: correlative groups such as NRTL [3], predictive groups such as UNIFAC [4] and its modification, COSMO-RS and COSMO-SAC [5], and semi-predictive

groups such as PC-SAFT [6] and NRTL-SAC [7] models. Currently, predictive models have limited capability and correlative models are not used in industry due to the lack of adjustable parameters for solute-solvent interactions. Until now, semi-predictive models have shown the best performance for predicting solubility. NRTL-SAC, which was introduced by Chen and Song [7], uses solubility data in a few solvents to predict solubility in a variety of solvents. Many applications of this model can be found in the literature for describing solubility data. Mota *et al.* [8] used this model to estimate the solubility of some pharmaceutical compounds. They fitted the parameters of this model to four organic solvents and then predicted the solubility of the solid materials in water with acceptable accuracy. A comparison of this model with other thermodynamic models proved its robustness and accuracy. Diedrichs and Gmehling [9] compared the performance of several models for solubility modelling. They reported that the models can be ranked in the following ascending order (best model mentioned first) with regard to the calculability of solubility: NRTL-SAC, Pharma Mod. UNIFAC, COSMO-RS and ideal (the activity coefficient in this model is equal to one). Tung *et al.* [10] compared the performance of the NRTL-SAC model and the COSMO-SAC model for the calculation of solubility of some APIs. The results showed that the NRTL-SAC model demonstrates a better performance. Sheikholeslamzadeh and Rohani [11] compared the NRTL-SAC model and the UNIFAC model for the calculation of solubility and again showed better results for the NRTL-SAC model. NRTL-SAC is a semi-predictive model that relies on experimental data. Results using this model have been shown to be better than those obtained from predictive models such as UNIFAC, COSMO-RS and COSMO-SAC.

The activity coefficient along the solubility curve can be determined experimentally from solubility data and solid state properties of the API. However, in supersaturated conditions, it is harder to measure the activity coefficient experimentally. Unfortunately there are only a handful of studies dealing with the experimental determination of the activity coefficient in conditions of supersaturation. Na *et al*. [12], using a sophisticated method (spherical void electrodynamics levitator trap), measured the water activity in supersaturated aqueous solutions of some amino acids. They observed that water activity at a constant temperature (25 °C) has a value of 6 for itaconic acid. Such a high activity ratio and consequently high activity coefficient ratio shows that the activity coefficient in supersaturation should be considered carefully in order to achieve an accurate estimation of driving force, and hence proper control of the crystal shape and size.

The fundamentals of the thermodynamics required in this project are presented in the sections below.

1.1 Definition of equilibrium and activity of a solid

Using supercooled liquid as a reference point, the chemical potential of solid, μ^{solid}, can be obtained as per equation 1-1, where μ^{liquid} is the chemical potential of the supercooled melt and a^{solid} is the activity of the solid:

$$\mu^{solid} = \mu^{liquid} + RT \ln a^{solid} \quad (1\text{-}1)$$

At equilibrium, the chemical potential of a solid is equal to the chemical potential of a solute:

$$\mu^{solid} = \mu^{solute} \quad (1\text{-}2)$$

Using the same reference for chemical potentials (that of a supercooled melt) in solid and solute gives equation 1-3, where a^{solid} is the activity of the solid, γ is the activity coefficient and x is the solubility:

$$a^{solid} = a^{solute} = \gamma x \quad (1\text{-}3)$$

Equation 1-3 shows that solubility can be estimated well if the activity of the solid is determined accurately and the activity coefficient calculated properly. The activity of a solid is related to Gibbs free energy of fusion, as outlined in equation 1-4:

$$\ln a^{solid} = \frac{-\Delta G^{fus}(T)}{RT} \quad (1\text{-}4)$$

Furthermore, the free energy of fusion is dependent on enthalpy and entropy:

$$\Delta G^{fus}(T) = \Delta H^{fus}(T) - T\,\Delta S^{fus}(T) \quad (1\text{-}5)$$

It can be shown through robust thermodynamics [13] that the activity of solid is equal to:

$$\ln a^{solid} = \frac{\Delta H^{fus}}{R}\left(\frac{1}{T_m} - \frac{1}{T}\right) + \frac{1}{R}\int_{Tm}^{T}\frac{\Delta C_p}{T}dT - \frac{1}{RT}\int_{Tm}^{T}\Delta C_p dT \quad (1\text{-}6)$$

where ΔC_p denotes the difference between the heat capacity of a supercooled melt and that of a solid.

1.2 Thermodynamics of the driving force

As mentioned above, driving force is related to the concentration ratio as well as the activity coefficient ratio. Figure 1-1 shows a plot of solubility (x) *versus* temperature (T):

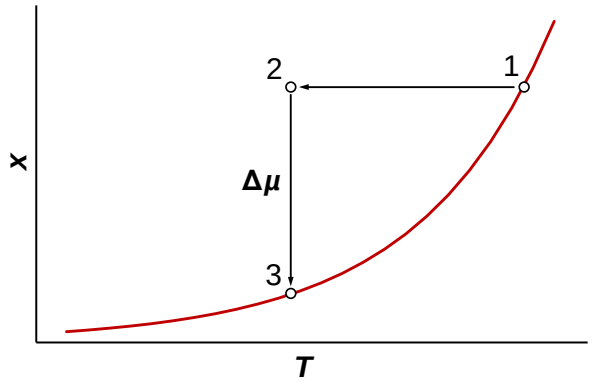

Figure 1-1. Diagram of cooling crystallisation

The driving force can be calculated as a ratio of activities:

$$\Delta\mu = \mu_2^{solute} - \mu_3^{solute} = RT_2 \ln \frac{a_2^{solute}}{a_3^{solute}} \quad (1\text{-}7)$$

Equation 1-7 can be shown as a ratio of composition and the activity coefficient:

$$\Delta\mu = RT_2 \ln \frac{x_2\gamma_2}{x_3\gamma_3} \quad (1\text{-}8)$$

where x_3 is the solubility of substance A in the solvent at temperature (T3) and x_2 is equal to the equilibrium solubility in point 1 (x_1). In order to obtain the driving force, solubility data at point 1 and point 3 are required as well as the activity coefficients at point 2 and point 3. The activity coefficient ratio is often assumed to be equal to one:

$$\Delta\mu \approx RT_2 \ln \frac{x_2}{x_3} \quad (1\text{-}9)$$

However, in many cases this is a poor assumption (as will be demonstrated later). One of the aims of this study was to compare the effect of composition and temperature on the activity coefficient, and from this analysis to answer the question “Can activity coefficients be used at point 1 instead of point 2 in equation 1-8?” The answer to this question is “yes” if the effect of temperature on the activity coefficient at a constant composition is much less than the effect of composition on the activity coefficient at a constant temperature.

1.3 Solubility

The solubility curve is determined experimentally or calculated theoretically. The solubility (x_2 and x_3) in Eq.1-8 can be calculated using thermodynamic models. These models calculate

the activity coefficient, and from the experimental determination of the activity of the solid, the solubility can be estimated using equation 1-3.

In thermodynamic models, the composition dependence of the activity coefficient is more pronounced than the temperature dependence. Some activity coefficient models entirely neglect the effect of temperature on the activity coefficient, such as in the case of the original NRTL-SAC model. Therefore one aim of this project was to incorporate the temperature-dependent parameter into the original NRTL-SAC model and compare its performance with that of the original NRTL-SAC model to calculate vapour liquid equilibria (VLE) and solid liquid equilibria (SLE). Furthermore, the prediction capability of the Pharma UNIFAC model was also evaluated during this project.

The NRTL-SAC and Pharma UNIFAC models are briefly introduced here. In the NRTL-SAC model, the molecule is divided into four conceptual segments and there is a binary interaction parameter between each pair of segments. The four segments are named as follows: X as hydrophobic, Y- as polar attractive, Y+ as polar repulsive and Z as hydrophilic. The interaction parameters between segments *i* and *j* are defined as τ_{ij} and τ_{ji}. An additional parameter named $r_{m,I}$ shows the amount of segment *m* in component *I*.

As stated previously, the original NRTL-SAC model is temperature independent. In this project, the original NRTL-SAC model was modified by incorporating a temperature-dependent binary interaction parameter:

$$\tau_{ij} = \frac{b_{ij}}{RT} \tag{1-10}$$

where b_{ij} shows the interaction between segment *i* and segment *j*.

In the Pharma UNIFAC model, a solution is considered as a mixture of functional groups rather than a mixture of molecules. The model is derived from the modified UNIFAC model through the introduction of additional functional groups and binary interaction parameters relevant for pharmaceutical molecules. There are three sets of parameters: binary interaction parameters between each pair of functional groups, and two parameters R_k and Q_k for each functional group.

There is a need for experimental determination of solubility since solubility has a direct effect on the thermodynamic driving force of crystallisation, and hence on crystal shape and size. In

this study, the solubility of two compounds – tolbutamide (Form II) and butamben (Form I) – in a range of solvents and at different temperatures was determined experimentally.

Tolbutamide is a first-generation sulfonylurea oral hypoglycaemic drug compound used in the treatment of type II diabetes. It has at least six polymorphs [14] and Form II is the most stable form at room temperature. The molecular structure of tolbutamide is shown in Figure 1-2.

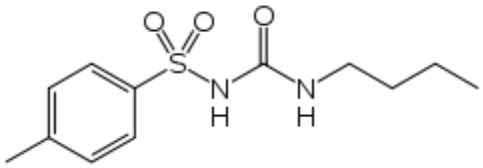

Figure 1-2. Diagram of a tolbutamide molecule

Butamben is generally used for topical treatment and for treating pain. The solid state characterisation of butamben was examined by Schmidt [15] and the compound was found to exist in two polymorphic structures. The author reported that Form I is the thermodynamically stable form at room temperature. The transition temperature from Form II to Form I is between 8 and 12 °C. The molecular structure of butamben is shown in Figure 1-3.

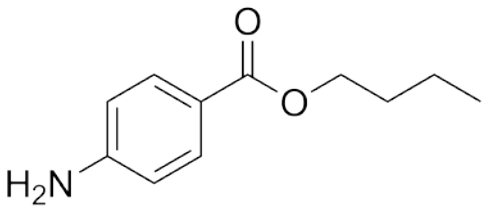

Figure 1-3. Diagram of a butamben molecule

1.4 Aims and objectives

The main aim of this study in particular is the investigation on solubility of APIs and the magnitude of the activity coefficient along the solubility curve. These two parameters are strongly related since for the same API, solubility increases with a decrease in the activity coefficient and *vice versa* (for a positive deviation from ideality). If a negative deviation from ideality occurs in solution, solubility increases with an increase in the activity coefficient. It is worth noting that a positive deviation from ideality mostly occurs in solutions. Knowledge of the solid-state properties of the compound together with its solubility data make it possible to

determine the activity coefficient in solution. Given that the activity coefficient and solubility are strongly related, the purpose of this study was to investigate in particular the effect of several parameters on solubility and the activity coefficient. For this purpose, the first objective is to investigate the effects of temperature and composition on the activity coefficient. The second objective is exploring the effect of temperature and type of solvent on solubility. And finally the last objective is to investigate the capability of the thermodynamic methods (NRTL-SAC and Pharma UNIFAC) to predict solubility. Aforementioned objectives of this work are given in more details in below:

1- The driving force of crystallisation is dependent on the concentration ratio as well as on the activity coefficient ratio. The concentration ratio and activity coefficient can be determined well experimentally along the saturation line, but the activity coefficient is a difficult property to measure experimentally in supersaturation conditions. In this project, an approach to calculate the driving force of crystallisation based solely on solubility data and solid-state properties of the compound was probed. Since the activity coefficient is dependent on both concentration and temperature, a good knowledge of the concentration and temperature dependence of the activity coefficient was required, therefore the influence of composition and temperature on the activity coefficient based on 30 binary VLE data was investigated.

2- The experimental determination of solubility is costly and tedious and thus there is a need for the prediction of solubility. In this project, the NRTL-SAC model, which is currently the best model for solubility prediction, was modified by incorporating a temperature-dependent parameter in order to ensure a more accurate prediction of the solubility of APIs in pure solvents.

3- Solubility has a considerable effect on the calculation of the thermodynamic driving force, yield of crystallisation *etc*. Therefore this study reports on the solubility of two APIs, tolbutamide and butamben, in a range of solvents at different temperatures. Furthermore, the thermodynamics of butamben in solution were investigated in detail.

Chapter 2 presents the investigation of the influence of temperature and composition on the activity coefficient. In Chapter 3, the solubility of some APIs was predicted by employing three models: “original NRTL-SAC”, “temperature-dependent NRTL-SAC” and “Pharma UNIFAC”. In Chapter 4, the solubility determination of two APIs, tolbutamide and

butamben, is presented and the thermodynamics of butamben studied in detail. Finally conclusions are discussed in Chapter 5.

Chapter 2: Improving estimates of crystallisation driving forces

In this chapter, the magnitude of temperature and composition dependence on activity coefficient is investigated. With reference to Figure 1-1, a critical analysis was used to determine whether the activity coefficient at point 2 is approximately equal to point 1.

Using SLE data, it is not possible to distinguish between the effect of temperature and the effect of composition on the activity coefficient. Therefore, VLE data were used to allow a comparison between the influence of temperature and composition on the activity coefficient. A new methodology to obtain the driving force of crystallisation was proposed. This method improved the estimation of the crystallisation driving force.

2.1 Methods

The DECHEMA dataset [16] was used to obtain the activity coefficient. Only data that met the following conditions were used:

i) experimentally determined isothermal VLE data were available at three or more temperatures

ii) all data were thermodynamically consistent, as verified by the method of van Ness *et al.* [17]

All the binary mixtures studied in this work are presented in Table 1.

Table 1. VLE data used in this work together with original references

Component 1	**Component 2**	**Temperatures [°C]**	**References**
Aqueous-organic systems			
Water	Acetaldehyde	10, 15, 20, 25, 30, 35, 40	[18]
Water	Ethanol	40, 55, 70	[19]
Water	1-propanol	30, 49.92, 60, 65.94, 79.80, 90	[20-23]
Water	2-propanol	35, 45, 55, 65	[23]
Water	Pyridine	50, 69.86, 80, 89.93	[24-25]
Polar-polar organic systems			
Methanol	Ethyl acetate	40, 50, 55, 60	[25-26]

Acetone	Methanol	55, 35, 45	[27-28]
Methyl acetate	Methanol	20, 30, 40, 49.76	[29-30]
Acetone	Ethanol	32, 40, 48	[31]
Chloroform	Ethanol	35, 45, 55, 60	[32-33]
Ethyl acetate	Ethanol	40, 55, 60, 70	, [3419]
Polar-nonpolar organic systems			
Cyclohexane	Ethanol	10, 20, 35, 50, 65	[35]
Diethyl ether	Ethanol	0, 10, 20, 30, 40, 50	[36]
Ethanol	Toluene	35, 45, 50, 55, 65, 70, 75	[37-38]
Ethanol	Benzene	25, 40, 45, 50, 55	[39-41]
Ethyl acetate	Benzene	50, 55, 60, 70	[42-43]
Toluene	Acetic acid	30, 69.94, 80.05	[44]
Nonpolar-nonpolar organic systems			
Diisopropyl ether	Benzene	50, 60, 70	[45]
Tetrachloromethane	Benzene	10, 20, 30, 40, 50, 60, 70	[46-49]
Benzene	Hexafluorobenzene	30, 40, 50, 60, 70	[50]
Tetrachloromethane	Toluene	35, 40, 45, 55, 65	[51]
Hexafluorobenzene	Toluene	30, 40, 50, 60, 70	[49]
Hexafluorobenzene	*p*-xylene	30, 40, 50, 60, 70	[50]
Benzene	Heptane	20, 45, 55, 80	[52-54]
Heptane	MEOK	65, 80, 95	[55]

In this work, the Van Laar equation was used to fit the activity coefficient data:

$$\ln \gamma_1 = A_{12}\left(\frac{A_{21}x_2}{A_{12}x_1 + A_{21}x_2} \right) \tag{2-1}$$

Despite its simplicity, it follows the Gibbs-Duhem relation applied to binary systems:

$$x_1\left(\frac{\partial \ln \gamma_1}{\partial x_1} \right)_{T,P} = x_2\left(\frac{\partial \ln \gamma_2}{\partial x_2} \right)_{T,P} \tag{2-2}$$

In order to investigate the influence of temperature on the activity coefficient, the activity coefficient at each temperature and at different compositions (x_i = 0.05, 0.20, 0.40, 0.60, 0.80, and 0.95) was calculated first. Subsequently, with each composition the activity coefficient was correlated with the linear equation (2-3) with respect to temperature.

$$\ln \gamma_i = a + bT \tag{2-3}$$

From eq. 2-3, b can be expressed as $(\partial \ln\gamma/\partial T)_x$. In most cases, the temperature dependence of the activity coefficients can be expressed by eq 2-3 with R^2 values more than 0.7. b was then correlated to the composition with a third order polynomial.

$$\left(\frac{\partial \ln \gamma_i}{\partial T} \right)_x = c + dx + ex^2 + fx^3 \tag{2-4}$$

Composition derivatives of the activity coefficient, $\left(\frac{\partial \ln \gamma_i}{\partial \ln x_i} \right)_T$ and $\left(\frac{\partial \ln \gamma_i}{\partial x_i} \right)_T$ were calculated at x_i=0.025, 0.125, 0.7 and 0.875 to investigate the influence of composition on the activity coefficient. In order to use just one value of $\left(\frac{\partial \ln \gamma_i}{\partial \ln x_i} \right)_T$ and $\left(\frac{\partial \ln \gamma_i}{\partial x_i} \right)_T$, T=298 K was used as a reference temperature since most solubility data are reported at or near this temperature.

2.2 RESULTS AND EVALUATION

Based on the procedure outlined in the Methods sections, an investigation was conducted on the influence of temperature and composition on the activity coefficient. The results showed that out of 30 binary mixtures, three systems showed a negative deviation from Raoult's law: hexafluorobenzene-benzene, hexafluorobenzene-toluene and hexafluorobenzene-*p*-xylene.

The other 27 binary mixtures showed a positive deviation from Raoult's law. In most cases, the composition dependence of γ_i at constant temperature followed a nonlinear approach toward unity. An example of this is illustrated in Figure 2-1. Out of 60 components from 30 binary mixtures, the activity coefficient at constant composition increased with increasing temperature over the whole concentration range for 13 components and decreased with increasing temperature for 31 components. For the remaining 16 cases, the temperature dependence of the activity coefficient was not uniform. For six binary systems, the activity coefficients of both components increased and for 14 systems they decreased with increasing temperature over the whole range of compositions. For six binary systems, the activity coefficients for both components increased in some ranges of the composition and decreased in others. For four systems, the activity coefficient of one component either increased or decreased with temperature over the whole range of composition, while for the other component it increased in one part of the composition range and decreased in another.

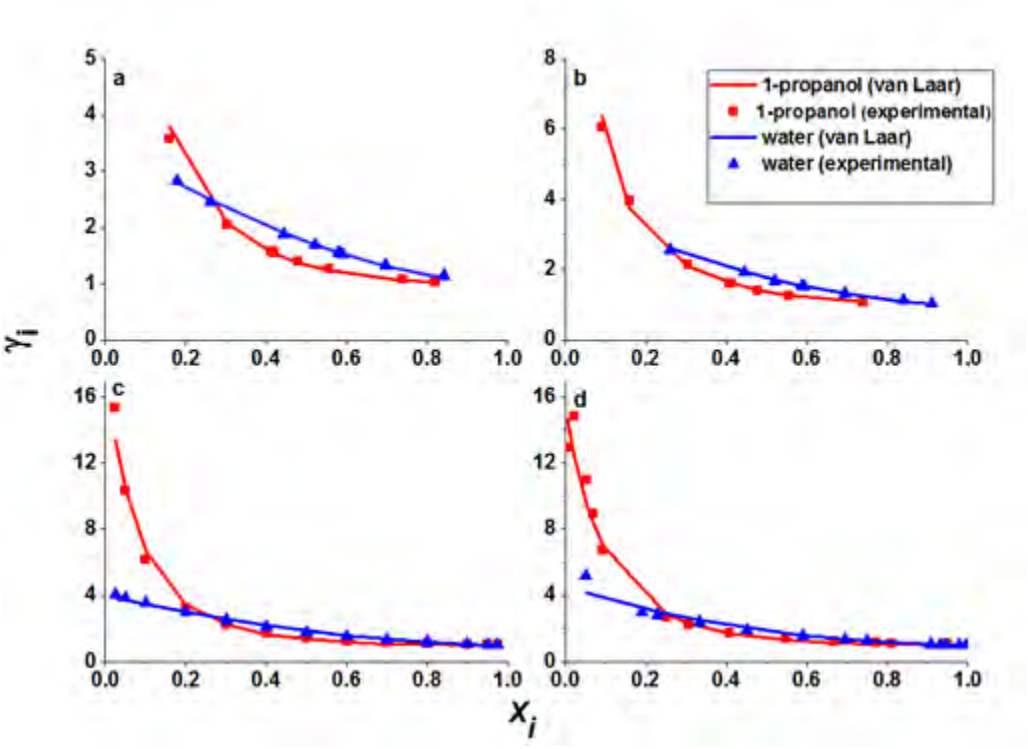

Figure 2-1. Activity coefficients of 1-propanol and water in a binary mixture of different compositions at four temperatures (symbols), and van Laar regression curves (lines): (a) T = 30 °C, (b) T = 50 °C, (c) T = 60 °C, (d) T = 66 °C

The results showed that the greatest influence of temperature on the activity coefficient occurred in the dilute range. In the following sections, the effect of temperature and

composition on the activity coefficient is discussed for each type of system (aqueous-organic, organic polar-polar, organic polar-nonpolar and organic nonpolar-nonpolar systems).

2.2.1 Aqueous-organic systems

Of the six binary mixtures included in this type, four systems induced a sign-change of the temperature derivative $(\partial \ \ln\gamma_i/\partial T)_x$ over the composition range, *i.e.* for some constant compositions, the activity coefficient decreased while for others it increased with increasing temperature.

The temperature derivative of the activity coefficient at constant composition and the composition derivative of the activity coefficient at constant temperature for the acetaldehyde-water system are plotted in Figure 2-2.

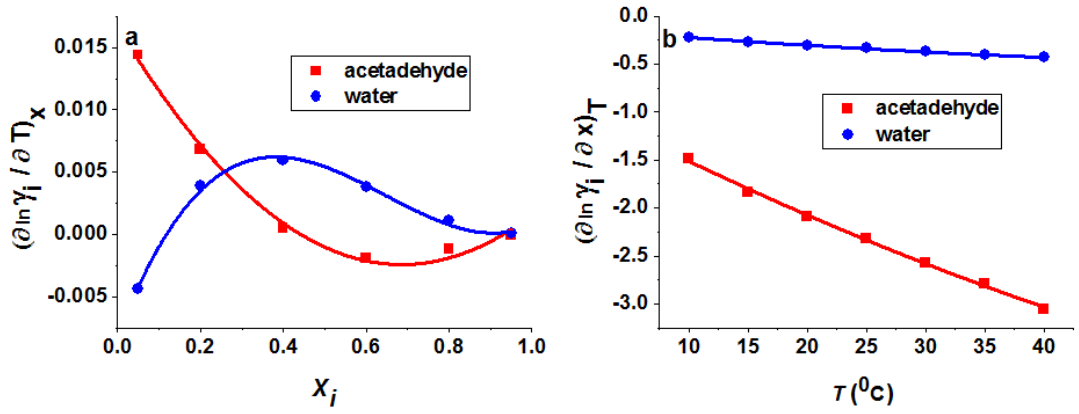

Figure 2-2. (a) Temperature derivative of the activity coefficient at constant composition as a function of composition; (b) composition derivative of the activity coefficient *versus* temperature for the acetaldehyde-water system

As shown in Figure 2-2b, the composition derivative of the activity coefficient for both components (acetaldehyde and water) is linear and the absolute value increases with increasing temperature. The composition derivative has a negative value since this system shows a positive deviation from Raoult's law. From this figure it is evident that the composition derivative of water is less than the composition derivative of acetaldehyde.

2.2.2 Nonpolar-nonpolar organic systems

Hexafluorobenzene-cyclohexane is representative of all nonpolar-nonpolar binary systems in the case of the temperature dependence of the activity coefficient. A plot of the temperature derivative of the activity coefficient at constant composition and of the

composition derivative of the activity coefficient at a constant temperature for this system is depicted in Figure 2-3. Figure 2-3(b) shows that the composition derivative of the activity coefficient follows a second-order polynomial trend. For both components, the composition derivative of the activity coefficient (absolute value) decreased and tended towards zero with increasing temperature.

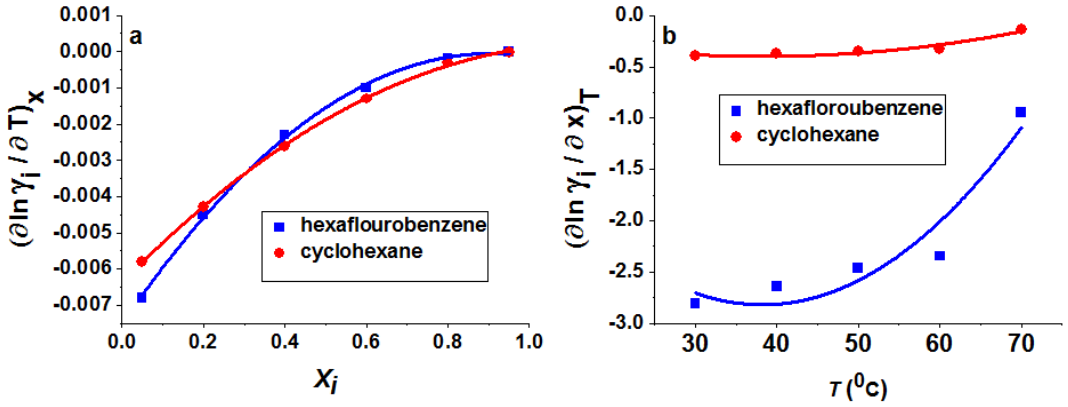

Figure 2-3. (a) Temperature derivative of activity coefficients at constant compositions as a function of composition; (b) composition derivative of activity coefficients at constant temperature as a function of temperature for the hexafluorobenzene–cyclohexane system

2.2.3 Polar-nonpolar organic systems

For polar-nonpolar organic systems, no general trend was found for the temperature derivative of the activity coefficient for the six binary mixtures studied in this project. Figure 2-4(a) shows how the temperature derivative of the activity coefficient at constant composition depends on the composition of the ethyl ether-ethanol system. Figure 2-4(b) shows the composition derivative of the activity coefficient at a constant temperature for the same system.

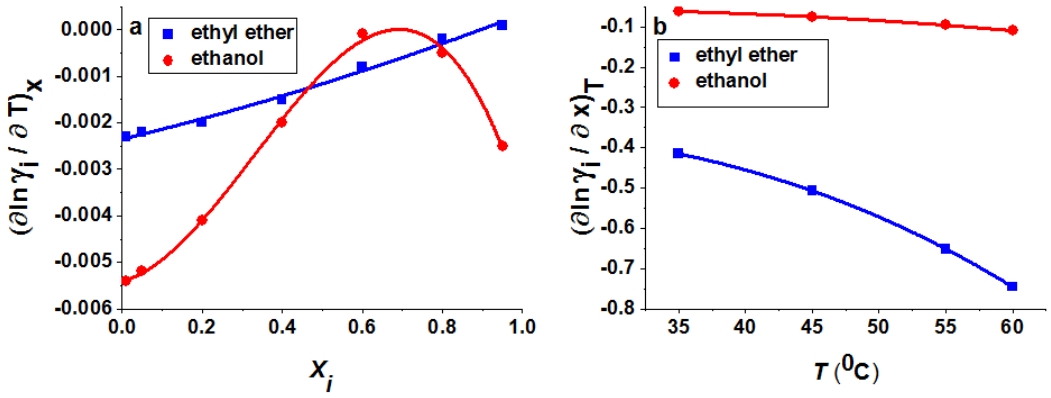

Figure 2-4. (a) Temperature derivative of the activity coefficient at constant temperature as a function of the composition of ethyl ether-water; (b) composition derivative of the activity coefficient at a constant temperature as a function of temperature for the ethyl ether-ethanol system

In the case of ethyl ether (Fig. 2-4b), the composition derivative of the activity coefficient seemed to follow a second-order polynomial. However, in the case of ethanol, it was a more linear relationship. This figure also shows that the activity coefficient of ethyl ether is more dependent on composition in comparison to ethanol.

2.2.4 Polar-polar organic systems

For most of the six polar-polar systems studied in this work, the activity coefficients (absolute value) decreased with increasing temperature. An example is shown in Figure 2-5(a) for the system methyl acetate-methanol. A plot of the composition derivative of the activity coefficient is constructed in Figure 2-5(a).

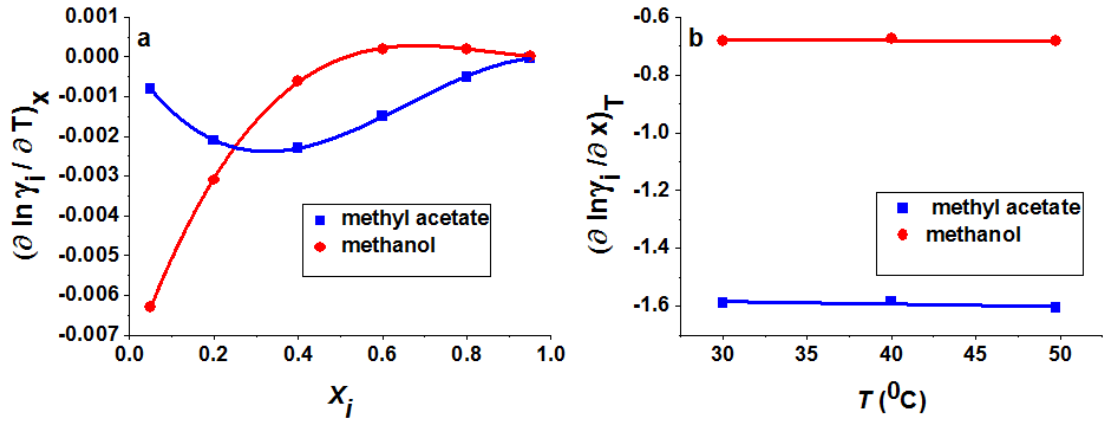

Figure 2-5. (a)The temperature derivative of the activity coefficient at constant composition as a function of composition of methyl acetate-methanol; (b) the composition derivative of the activity coefficient as a function of temperature for the methyl acetate-methanol system

As shown in Figure 2-5 (a), the composition derivative of the activity coefficient at a constant temperature is negative, indicating a positive deviation from Raoult's law for both components. It is also evident from this figure that the composition derivative of the activity coefficient is very weakly dependent on temperature.

Since the mole fraction is a normalised parameter, the temperature was also changed to a normalised parameter in order to accurately compare the effect of temperature and the effect of composition.

Normalised temperature is defined as per Eq. 2-5:

$$\theta = \frac{T - T_{low}}{T_{up} - T_{low}} \tag{2-5}$$

where T_{low} and T_{high} refer to the boiling points of the pure components at normal pressure boiling points.

In Figure 2-6, the ratio of the composition derivative of the activity coefficient at constant temperature to that of the normalised temperature derivative of the activity coefficient at constant composition is depicted. 30 binary mixtures resulted in 60 data points (since each binary mixture contained two components). The compositions investigated for this analysis were x_i=0.025, 0.125, 0.7 and 0.875.

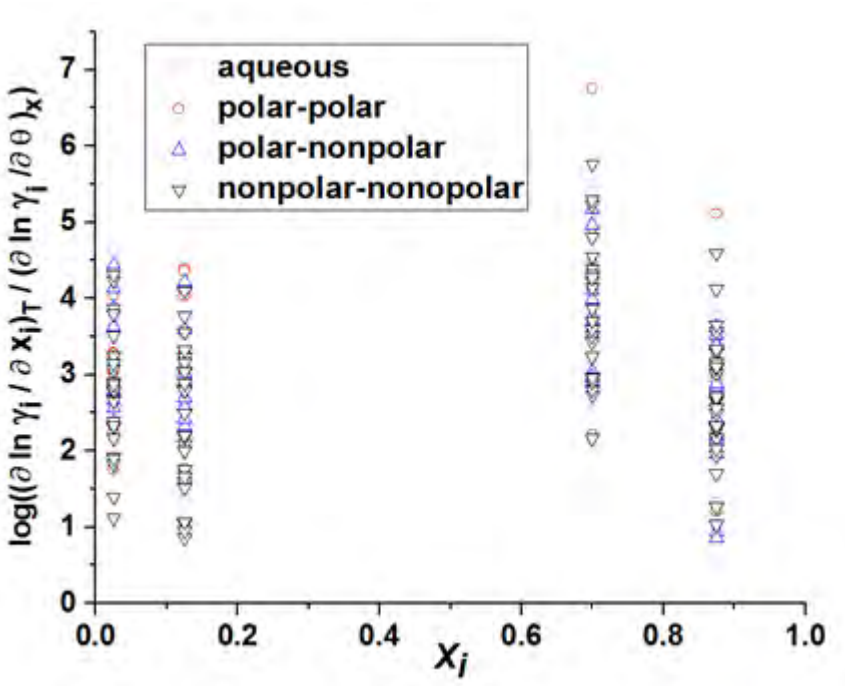

Figure 2-6. Comparison of temperature and concentration dependence of the activity coefficient

Figure 2-6 demonstrates that the log value (ratio of derivatives) was greater than 1 in most cases, which shows that the influence of temperature on the activity coefficient is at least ten times less than the influence of composition.

2.3 DISCUSSION AND ANALYSIS

Since the activity coefficient depends on temperature and composition, the total derivative of the activity coefficient can be expressed as:

$$d\ln\gamma = \left(\frac{\partial \ln\gamma}{\partial x}\right)_T dx + \left(\frac{\partial \ln\gamma}{\partial T}\right)_x dT \qquad (2\text{-}6)$$

By dividing all terms by dT in the case of VLE, this gives:

$$\left(\frac{d\ln\gamma}{dT}\right)_p = \left(\frac{\partial \ln\gamma}{\partial x}\right)_T \left(\frac{\partial x}{\partial T}\right)_P + \left(\frac{\partial \ln\gamma}{\partial T}\right)_x \qquad (2\text{-}7)$$

In order to analyse this equation, a binary mixture of nine VLE systems was used. Figure 2-7 shows a plot of $\left(\frac{\partial \ln\gamma}{\partial \ln x}\right)_T \left(\frac{\partial \ln x}{\partial T}\right)_P$ on the x-axis *versus* $\left(\frac{\partial \ln\gamma}{\partial T}\right)_x$ on the y-axis.

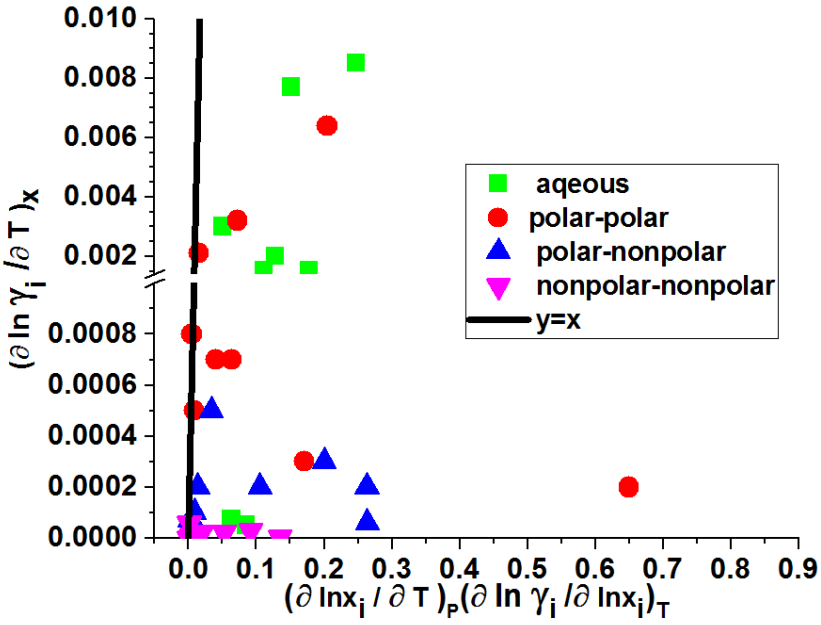

Figure 2-7. Comparison between the influence of temperature and composition on the activity coefficient for four compositions, x = 0.025, 0.125, 0.7 and 0.875, using VLE data for methanol-water [56], ethanol-water [57], methanol-methyl acetate [58], ethanol-benzene [59], benzene-diisopropylether [60], ethyl acetate-benzene [61] and benzene-tetracholomethane [62]

As shown in Figure 2-7, $\left(\frac{\partial \ln \gamma}{\partial \ln x}\right)_T \left(\frac{\partial \ln x}{\partial T}\right)_P$ is clearly higher than $\left(\frac{\partial \ln \gamma}{\partial T}\right)_x$.

Another form of equation 2-7 is shown in equation 2-8:

$$\frac{\left(\frac{d \ln \gamma}{dT}\right)_{eq}}{\left(\frac{\partial \ln \gamma}{\partial T}\right)_x} = \frac{\left(\frac{\partial \ln \gamma}{\partial \ln x}\right)_T}{\left(\frac{\partial \ln \gamma}{\partial T}\right)_x}\left(\frac{\partial \ln x}{\partial T}\right)_p + 1 \qquad (2\text{-}8)$$

Then if:

$$\frac{\left(\frac{\partial \ln \gamma}{\partial \ln x}\right)_T}{\left(\frac{\partial \ln \gamma}{\partial T}\right)_x} \rangle\rangle \frac{1}{\left(\frac{\partial \ln x}{\partial T}\right)_p} \qquad (2\text{-}9)$$

Eq. 2-9, if true, shows that the influence of composition on the activity coefficient is much higher than the influence of temperature. In order to analyse this equation, the left-hand and right-hand terms were plotted against concentration in Figure 2-8 at x_i = 0.025, 0.125, 0.7 and 0.875.

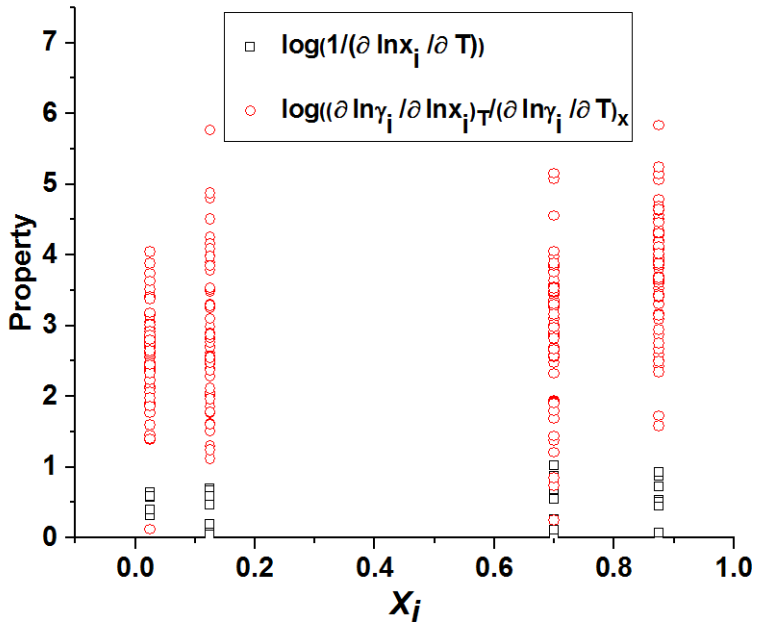

Figure 2-8. Comparison between $\frac{1}{\left(\frac{\partial \ln x}{\partial T}\right)_p}$ and the ratio of the concentration derivative of the activity coefficient to the temperature derivative of the activity coefficient

Figure 2-8 clearly shows that the influence of temperature on the activity coefficient is much less than the influence of composition, and finally since:

$$\Delta H^{mix} = -RT^2\left(\frac{\partial \ln \gamma}{\partial T}\right)_x \qquad (2\text{-}14)$$

The enthalpy of mixing is positive in a positive deviation from ideality. Therefore in this case the temperature derivative of the activity coefficient at constant composition is negative. In a negative deviation from ideality, the enthalpy of mixing is negative and therefore the temperature derivative is positive.

Since a positive deviation was seen in most cases in SLE, it can be expected that the activity coefficient at constant composition decreases with increasing temperature. Furthermore, equation 2-14 shows that as a system deviates further from ideality, the temperature derivative increases. Furthermore, for the same compound in different solvents, the temperature derivative of the activity coefficient at constant composition was found to be higher for the solvent in which the solubility was lowest.

Chapter 3: Solubility prediction

This chapter focuses on solubility calculations for five APIs using temperature-dependent NRTL-SAC and original NRTL-SAC. In addition, the solubility prediction of Pharma UNIFAC was evaluated for three APIs.

3.1 Modelling work

3.1.1 Model API substances

All the APIs studied in this work are presented in Figure 3-1.

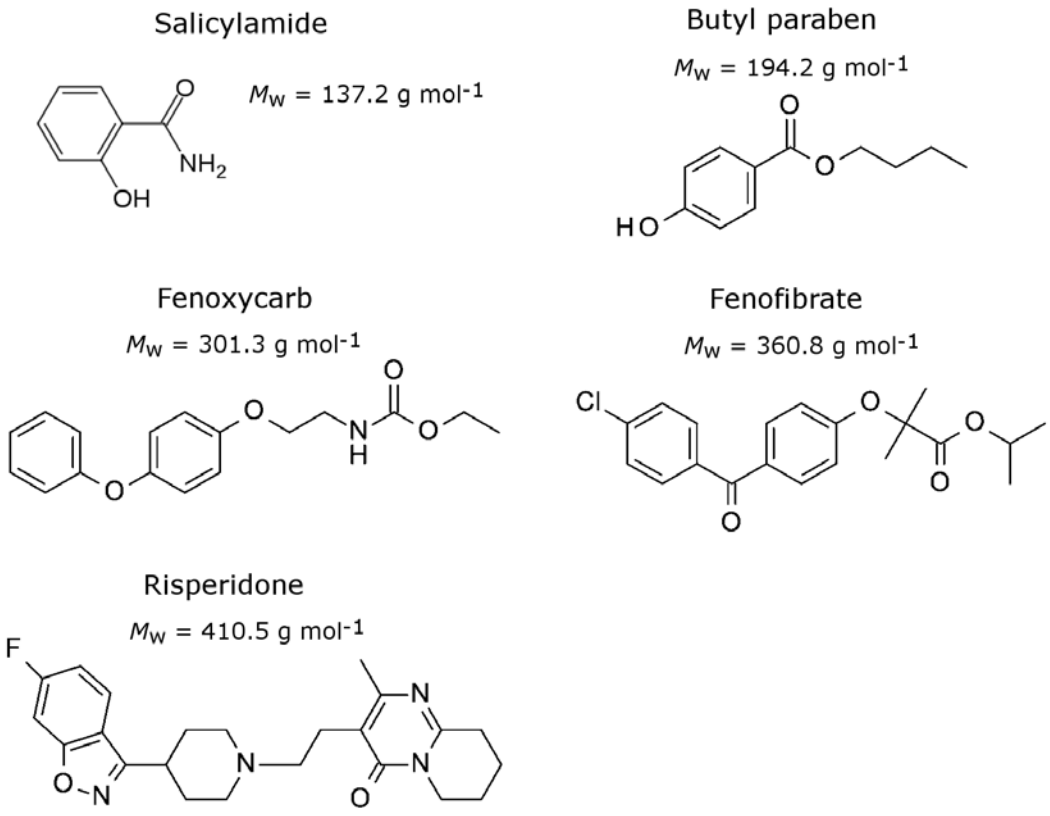

Figure 3-1. Model API compounds

The heat capacity difference between super-cooled melt and solid is correlated in the literature by the following equation:

$$\Delta C_p = q + r(T - T_m) \tag{3-1}$$

All the data needed to calculate the activity of the solid are given in Table 3-1.

Table 3- 1. Calorimetric data for the model API compounds

Compound	T_m / K	$\Delta^{fus}H(T_m)$ / kJ mol^{-1}	q / J K^{-1} mol^{-1}	r / J K^{-2} mol^{-1}	References
Salicylamide	411.9±0.5	29.0±0.3	192.3	0.9322	[63]
Butyl paraben	340.5±0.4	26±1.4	77.2	0.490	[64]
Fenoxycarb	326.3	26.98	106.5	0.0424	[65-66]
Fenofibrate	352.05±0.02	33.5±0.6	124.3	0.5192	[13]
Risperidone	442.4±0.3	43.9±0.2	158.1	0.5214	[67]

3.1.2 The NRTL-SAC model

In this model, a solution is treated as a mixture of molecular segments. Each molecule is described in terms of four different segments and segment-segment binary interaction parameters have been introduced. The four segments are labelled as follows: X for the hydrophobic, Y- for the polar attractive, Y+ for the polar repulsive and Z for the hydrophilic segment. The hydrophobic segment represents the molecular surface area that is unlikely to form hydrogen bonds, the hydrophilic segment represents the area with interactions likely to form hydrogen bonds, and the polar segment represents the area with interactions characteristic of an electron donor or acceptor. For each pair of different segments i and j, there are two dimensionless binary interaction parameters, denoted τ_{ij} and τ_{ji}, and the amount of a segment in a molecule is given by a parameter called the segment number, $r_{m,I}$, for segment type m in molecule I.

In this model, the activity coefficient is the sum of two terms, the combinatorial and residual contributions:

$$\ln \gamma_I = \ln \gamma_I^C + \ln \gamma_I^R \qquad (3\text{-}2)$$

In the above equation, the combinatorial part is related to the difference between the shape and size of the molecule, while the residual part is related to the interaction between the molecules, which can be obtained by:

$$\ln \gamma_I^R = \sum_m r_{m,I} \left(\ln \Gamma_m^{lc} + \ln \Gamma_m^{lc,I} \right) \qquad (3\text{-}3)$$

Γ_m^{lc} denotes the (local composition) activity coefficients of segment *m*, and $\Gamma_m^{\mathrm{lc},I}$, the activity coefficient of segment *m* within component *I.* The two terms can be expressed as:

$$\ln \Gamma_m^{lc,I} = \frac{\sum_j x_{j,I} G_{jm} \tau_{jm}}{\sum_k x_{k,I} G_{km}} + \sum_{m'} \frac{x_{m',I} G_{mm'}}{\sum_k x_{k,I} G_{km'}} \left(\tau_{mm'} - \frac{\sum_j x_{j,I} G_{jm'} \tau_{jm'}}{\sum_k x_{k,I} G_{km'}} \right) \tag{3-4}$$

$$\ln \Gamma_m^{lc} = \frac{\sum_j x_j G_{jm} \tau_{jm}}{\sum_k x_k G_{km}} + \sum_{m'} \frac{x_{m'} G_{mm'}}{\sum_k x_k G_{km'}} \left(\tau_{mm'} - \frac{\sum_j x_j G_{jm'} \tau_{jm'}}{\sum_k x_k G_{km'}} \right) \tag{3-5}$$

$$G_{ij} = \exp\left(-\alpha \tau_{ij}\right) \tag{3-6}$$

All equations for the original NRTL-SAC are presented in Chen and Song [7]. The indices *j, k, m* and *m′* can show each of the segment types (X, Y^+, Y^- and Z). x_j and $x_{j,I}$ are segment-based mole fractions of segment *j* in total and in component *I*, which are functions of the segment numbers and solution composition.

The original NRTL-SAC model considers that binary interaction parameters between each pair of segments are independent of temperature. However, in this project a temperature-dependent binary interaction parameter was utilised between each pair of segments according to:

$$\tau_{ij} = \frac{b_{ij}}{RT} \tag{3-7}$$

b_{ij} in the above equation represents the temperature-independent binary interaction parameter between segment *i* and segment *j*. There are 12 binary interaction parameters, however some assumptions are made: $\tau_{y^-z} = -\tau_{y^+z}$, $\tau_{zy^-} = \tau_{zy^+}$, $\tau_{xy^-} = \tau_{xy^+}$, $\tau_{y^-x} = \tau_{y^+x}$ and $\tau_{y^-y^+} = \tau_{y^+y^-} = 0$ (for the original, temperature-independent NRTL-SAC model) and $b_{y^-z} = -b_{y^+z}$, $b_{zy^-} = b_{zy^+}$, $b_{xy^-} = b_{xy^+}$, $b_{y^-x} = b_{y^+x}$ and $b_{y^-y^+} = b_{y^+y^-} = 0$ (for the temperature-dependent NRTL-SAC model).

Therefore, six parameters need to be determined when using the data for the reference solvents. The objective function used for fitting the binary interaction parameters was:

$$OF = \sum_{C=1}^{2} \sum_{N} \left(\gamma^{\exp} - \gamma^{\text{th}} \right)^2 \quad (3\text{-}8)$$

where $\gamma^{\exp}$ is the experimentally determined activity coefficient, γ^{th} is the activity coefficient calculated using NRTL-SAC, N is the number of data points and C is the component in the binary mixture.

For each solvent, there are four segments that can be obtained from VLE and for each solute. Four segments can also be obtained from SLE.

In order to obtain the parameters of the model, binary interaction parameters from the experimental data of each pair of three references solvents were first calculated. Between segments X and Z, τ_{xz} and τ_{zx} were determined by fitting to the binary VLE data [68] of hexane-water, a mixture that just has X and Z segments. Then, the binary interaction parameters between segments Z and Y^- and Y^+, $\tau_{zy^-}, \tau_{zy^+}, \tau_{y^+z}, \tau_{y^-z}$ and $b_{zy^-}, b_{zy^+}, b_{y^-z}, b_{y^+z}$, were determined by fitting to binary VLE data [68] for the system acetonitrile-water which contains only X, Y^- and Y^+ segments for acetonitrile and the Z segment for water. As there are no VLE data available for the system acetonitrile-hexane, binary interaction parameters between segments X and Y^- and Y^+, $\tau_{xy^-}, \tau_{xy^+}, \tau_{y^-x}, \tau_{y^+x}$, were equalled to the same values as in the original NRTL-SAC publication [7] where LLE data for the system acetonitrile-hexane were used.

In the case of the temperature-dependent NRTL-SAC model, the temperature-independent interaction parameters between segments X and Y^- and between X and Y^+, $b_{xy^-}, b_{xy^+}, b_{y^-x}, b_{y^+x}$, were obtained using:

$$\ln b_{ij} = \ln \tau_{ij(298\text{K})} + \ln 8.314 + \ln 298 \quad (3\text{-}9)$$

where $\tau_{ij(298\ \text{K})}$ denotes the binary interaction parameter at 298 K reported in the original NRTL-SAC publication [7].

In the next step the segment parameters for eight solvents were calculated. These solvents were as follows: 1-butanol, 1-propanol, 2-propanol, acetone, ethanol, ethyl acetate, methanol and toluene. VLE data in the DECHEMA dataset were used to calculate the segment numbers.

Experimental activity coefficient values were obtained by applying equation 3-10, by assuming ideal vapour phase behaviour and calculating pure component vapour pressures using the Antoine equation:

$$\gamma_I^{\exp} = \frac{y_I P}{x_I P_I^{\text{sat}}} \qquad (3\text{-}10)$$

In the last step the segment parameters for five APIs were determined. For this purpose the solubilities of the APIs in two solvents were first correlated, and one polar solvent (methanol) and one non-polar solvent (toluene, or when solubility data is not available, ethyl acetate) were used in order to determine segment parameters of the solute. The solubility of the APIs in the other solvents was then predicted.

Reported solubility data in toluene and methanol were used for risperidone [67] and fenoxycarb [69], and solubility data in methanol and ethyl acetate were used for fenofibrate [13], butyl paraben [70] and salicylamide [71].

Table 3-2 shows the binary interaction parameters between segments obtained for the original and temperature-dependent NRTL-SAC models. The binary interaction parameters between segments Y^- and Y^+ were set to zero as in the original model [7]. Segment parameters (r_X, r_{Y-}, r_{Y+} and r_Z) for each of the eight solvents and for the five APIs are listed in Table 3-3 for the original and the temperature-dependent NRTL-SAC models.

Table 3-2. Binary interaction parameters for the NRTL-SAC models

τ_{xz}	τ_{zx}	τ_{y+z}	τ_{y-z},	τ_{zy-}, τ_{zy+}	τ_{xy-}, τ_{xy+}	τ_{y-x}, τ_{y+x}
4.7334	0.1692	1.6884	-1.6884	1.7239	1.6430	1.8340
b_{xz}	b_{zx}	b_{y+z}	b_{y-z},	b_{zy-}, b_{zy+}	b_{xy-}, b_{xy+}	b_{y-x}, b_{y+x}
9795.42	4902.83	4247.45	-4247.45	4576.13	4070.65	4543.86

Table 3-3. Segment parameters of solvents and API solutes for the NRTL-SAC models.

Compound	*T*-dependent NRTL-SAC				Original NRTL-SAC			
	r_X	r_{Y-}	r_{Y+}	r_Z	r_X	r_{Y-}	r_{Y+}	r_Z
1-Butanol	1.1046	0.0012	1.9997	0.0001	0.9989	0.3818	1.6263	0.0019
1-Propanol	1.5663	0.7220	0.0007	2.1213	0.1681	0.0003	0.0056	0.8963
2-Propanol	0.1411	0.1430	0.0000	0.4935	1.3719	0.4942	0.0145	0.0006
Acetone	0.2852	0.0001	0.7782	0.0000	0.2661	0.1050	0.7000	0.0000
Ethanol	0.5784	0.0003	0.0002	0.8263	0.4466	0.0495	0.0008	0.9413
Ethyl acetate	1.0497	0.0003	1.5677	0.0004	0.7654	0.0949	1.1151	0.0005
Methanol	0.0008	0.7510	0.0000	0.0436	0.0004	0.0636	0.0006	0.5325
Toluene	1.0306	0.0250	0.5431	0.0005	1.0631	0.0003	0.4224	0.0000
Salicylamide	1.2196	0.0545	0.4666	0.1879	0.9642	0.0527	0.3096	0.3097
Butyl	0.0000	0.0122	0.5842	0.0733	3.0688	0.5597	3.5141	0.0020
Fenoxycarb	1.8467	0.2534	0.0681	0.3522	1.4204	0.0552	1.2732	0.1240
Fenofibrate	2.0107	0.1023	0.2713	0.1860	1.6541	0.0552	1.3544	0.0099
Risperidone	1.6799	0.1407	0.1410	0.6544	1.9122	1.7661	1.3203	0.4286

3.1.3 Pharma UNIFAC

Equations for the Pharma UNIFAC model are reported by Diedrichs and Gmehling [9]. In this model there are three kinds of parameters: binary interaction parameters between each pair of functional groups, and two parameters R_k and Q_k for each functional group. The functional groups for salicylamide are 4 × ACH, 1 × ACOH, and 1 × AC-$CONH_2$, for butyl paraben 1 × CH_3, 3 × CH_2, 4 × ACH, 1 × ACOH, and 1 × ACCO, and for fenoxycarb 1 × CH_3, 2 × CH_2, 1 × COO, 1 × CH_2NH, 2 × ACO, 9 × ACH, and 1 × C. It is worth noting that the Pharma UNIFAC model was not evaluated for fenofibrate and risperidone since parameters are not available for all the functional groups of these molecules.

3.2 Results and discussion

3.2.1 Comparison of original and temperature-dependent NRTL-SAC models for correlation of VLE data

The average relative deviation (ARD) between the experimental and calculated activity coefficients is given in Table 3-4. ARD is defined as:

$$ARD = \frac{1}{N}\sum_{N}\frac{\left|\gamma_I^{\exp} - \gamma_I^{\text{th}}\right|}{\gamma_I^{\exp}} \tag{3-11}$$

where I denotes the component and N is the number of data points.

It can be seen in Table 3-4 that in some cases the original NRTL-SAC model can correlate the activity coefficient in ARD less than the temperature-dependent model, but if the average error is taken for each solvent in all three cases, the temperature-dependent model produced more accurate results. Figure 3-2 shows the average error in Table 3-1 for each solvent.

Table 3-4. Average relative deviation (*ARD*) in activity coefficients for the NRTL-SAC models

Component 1	Component 2	*N*	*T*-range (K)	*ARD*			
				Original		*T*-dependent	
				γ_1	γ_2	γ_1	γ_2
Water	Hexane	17	363-473	0.18	0.06	0.15	0.06
Acetonitrile	Water	11	353-359	0.06	0.11	0.04	0.11
1-Butanol	Hexane	20	341-380	0.09	0.11	0.11	0.09
	Acetonitrile	14	354-390	0.26	0.41	0.28	0.43
	Water	28	372-384	0.25	0.12	0.03	0.03
1-Propanol	Hexane	16	336-350	0.30	0.60	0.24	0.37
	Acetonitrile	17	354-363	0.17	0.17	0.22	0.22
	Water	15	367-371	0.21	0.10	0.23	0.06
2-Propanol	Hexane	14	337-350	0.10	0.09	0.44	0.31
	Acetonitrile	15	351-354	0.23	0.22	0.27	0.33
	Water	26	354-372	0.39	0.33	0.04	0.03
Acetone	Hexane	9	324-332	0.03	0.01	0.02	0.02
	Acetonitrile	9	330-352	0.11	0.04	0.08	0.03
	Water	12	331-368	0.10	0.06	0.06	0.06
Ethanol	Hexane.	16	339-349	0.25	0.20	0.16	0.12
	Acetonitrile	3	293-323	0.66	0.27	0.44	0.22
	Water	12	351-369	0.29	0.27	0.25	0.23
Ethyl acetate	Hexane	3	353-355	0.02	0.12	0.06	0.04
	Acetonitrile	4	333-353	0.03	0.01	0.03	0.01
	Water	5	343-380	0.02	0.02	0.02	0.01
Methanol	Hexane	7	329-333	0.06	0.05	0.08	0.08
	Acetonitrile	21	314-323	0.24	0.22	0.07	0.09
	Water	8	339-369	0.57	0.17	0.46	0.11
Toluene	Hexane	5	293-313	0.70	0.11	0.72	0.14
	Acetonitrile	25	354-381	0.25	0.19	0.25	0.12
	Water	14	342-363	0.24	0.21	0.22	0.16

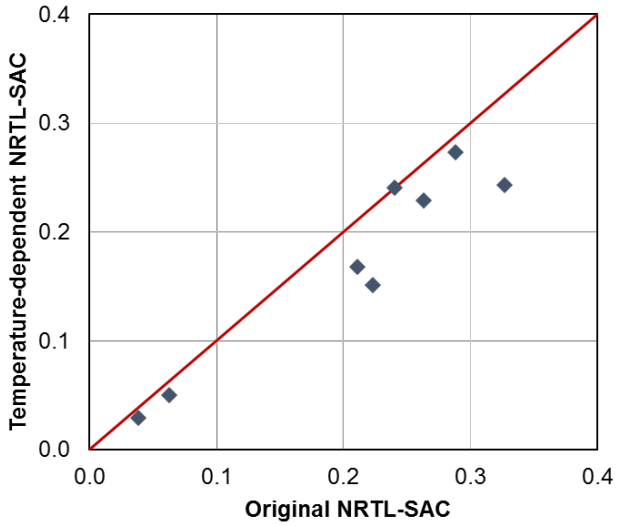

Figure 3-2. *ARD* in correlated activity coefficients *vs*. experimental values for the original and the temperature-dependent NRTL-SAC models. Each point represents the average *ARD* for both components in binary systems of one organic solvent in hexane, acetonitrile and water

3.2.2 Comparison of all three models for prediction of API solubility

In Table 3-5, the root mean squared logarithmic error (RMSLE) in calculated *vs*. experimental mole fraction solubility, equation 3-12, for each of the API-solvent systems is reported for each of the evaluated methods. Solvents used for parameter determination are marked with an asterisk (*):

$$RMSLE = \frac{\sqrt{\sum_{N} \left(\ln x_{\text{exp}} - \ln x_{\text{calc}}\right)^2}}{N} \tag{3-12}$$

In Figure 3-3, for each system, RMSLE values obtained with the temperature-dependent NRTL-SAC model and the Pharma UNIFAC model are plotted *vs*. values obtained with the original NRTL-SAC model.

Table 3-5. RMSLE in predicted mole fraction solubility for API-solvent systems for the three models

		RMSLE		
Compound	**Solvent**	**Pharma UNIFAC**	***T*-dependent NRTL-SAC**	**Original NRTL-SAC**
Salicylamide	Methanol*	1.63	0.01	0.02
	Ethyl acetate*	1.77	0.01	0.02
	Acetonitrile	1.01	0.34	0.65
	Acetone	1.37	0.53	0.54
	Water	9.34	3.45	4.62
Butyl paraben	Methanol*	1.25	0.03	0.09
	Ethyl acetate*	0.62	0.02	0.13
	Ethanol	0.18	0.42	1.12
	1-Propanol	0.30	0.38	0.29
	Acetonitrile	0.61	1.02	0.63
	Acetone	0.46	0.05	0.30
Fenoxycarb	Methanol*	1.08	0.05	0.12
	Toluene*	0.37	0.24	0.27
	Ethanol	1.08	0.70	1.06
	2-Propanol	2.16	1.67	1.78
	Ethyl acetate	0.36	0.29	0.81
Fenofibrate	Methanol*		0.03	0.13
	Ethyl acetate*		0.11	0.91
	Ethanol		0.59	1.70
	1-Propanol		1.42	1.36
	2-Propanol		2.87	2.79
	Acetonitrile		1.49	0.13
	Acetone		0.14	1.01
Risperidone	Methanol*		0.08	0.22
	Toluene*		0.15	0.15
	Ethanol		1.21	2.29
	1-Propanol		2.39	1.69
	2-Propanol		1.86	2.85
	1-Butanol		1.47	1.67
	Acetone		4.02	0.41
	Ethyl acetate		2.14	0.38

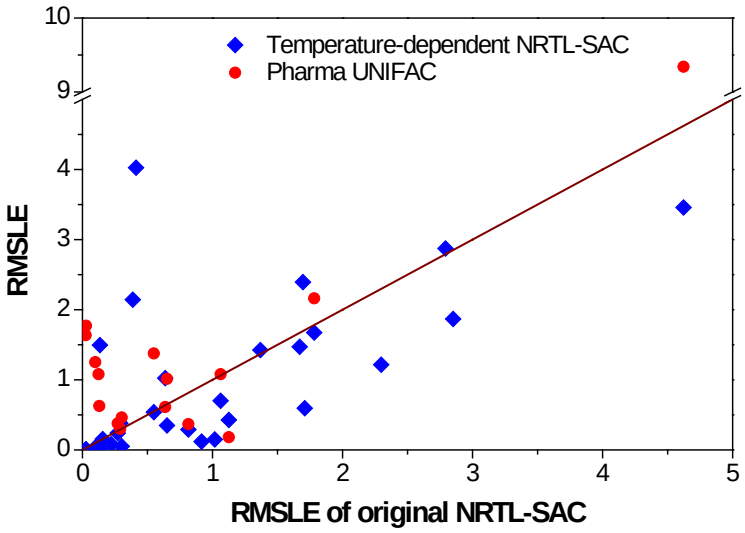

Figure 3-3. RMSLE in mole fraction solubilities predicted with the temperature-dependent NRTL-SAC and the Pharma UNIFAC models *vs*. the corresponding values obtained for the original NRTL-SAC model, for the systems listed in Table 3-5

In Figure 3-4 the experimental solubility of butyl paraben in four different solvents is compared with the solubility curves predicted using the three evaluated models.

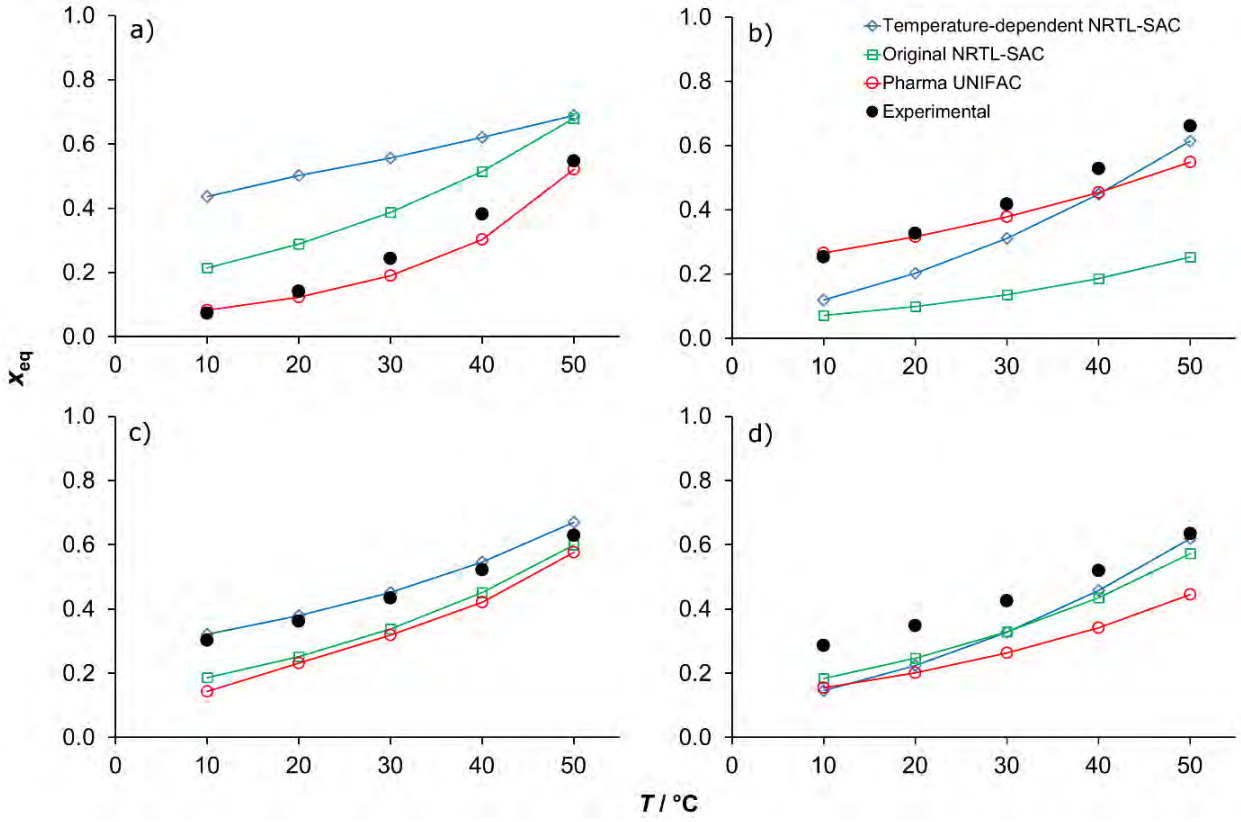

Figure 3-4. Predicted and experimentally determined solubility curves of butyl paraben in different solvents: a) acetonitrile, b) ethanol, c) acetone and d) 1-propanol

In terms of correlation, the average RMSLE values of the temperature-dependent and the original NRTL-SAC models were 0.07 and 0.21 respectively. For solubility prediction in other solvents, the average RMSLE of the two methods was very similar at 1.35 and 1.34 respectively. However when the average across all solvents for each API was calculated, except for risperidone, the temperature-dependent NRTL-SAC model produced more accurate results than the original NRTL-SAC model. Table 3-5 shows that the temperature-dependent model produced better results than the original model in 23 out of 31 cases, including all salicylamide and fenoxycarb systems.

The complexity of an API can be shown by molecular weight. Figure 3-5 shows a RMSLE value averaged across the different solvents for each API, for the three evaluated models, with solute molecular weight on the *x*-axis.

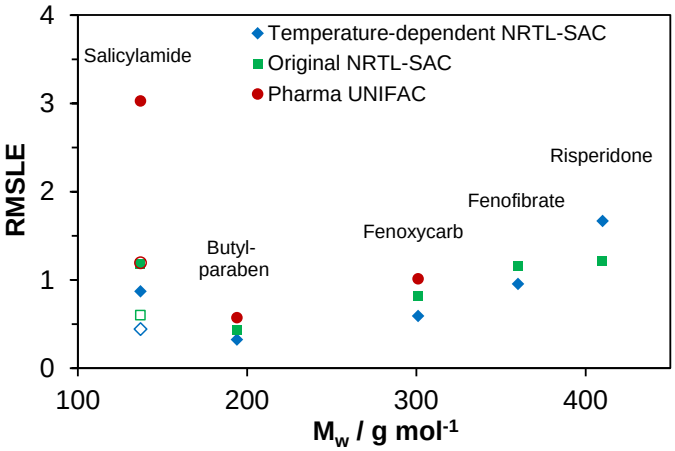

Figure 3-5. RMSLE of predicted solubilities averaged across different solvents for each API, shown for the three different models as a function of molecular weight. For salicylamide, hollow symbols represent averages excluding water

For each of the APIs evaluated by Pharma UNIFAC, both NRTL-SAC models showed a better performance, with the most pronounced difference being seen for salicylamide. It is notable that the prediction results for this compound in water are about an order of magnitude worse than those of the organic solvents. In Figure 3-5, the hollow symbols for salicylamide represent data averaged over the organic solvents only. As can be seen in Figure 3-5, for the NRTL-SAC models there is a good correlation between prediction error and molecular weight.

Indeed if more solvents for the calibration of NRTL-SAC were used, better results in terms of prediction could be expected. In order to examine this, segment parameters were re-

determined for the temperature-dependent NRTL-SAC model for one API, salicylamide, this time using data in four solvents (methanol, ethyl acetate, acetone and acetonitrile). Using the new segment parameters of r_x=0.8188, r_{y-}=0.1391, r_{y+}=0.8842 and r_z=0.1012, the RMSLE in predicted solubility in water was reduced from 3.5 to 2.6.

It was shown that the introduction of a simple inverse temperature-dependence to the binary interaction parameters of the NRTL-SAC activity coefficient model led to an improvement in the performance of this model for the correlation of vapour-liquid as well as solid-liquid equilibrium data.

Furthermore, the results showed that for prediction of the solubility of pharmaceutical compounds in organic solvents, the temperature-dependent form of NRTL-SAC results in an improvement in accuracy compared with the original form of the model, while both models were more accurate than Pharma UNIFAC. For an evaluated set of pharmaceutical compounds, the accuracy of both NRTL-SAC models was shown to deteriorate with increasing solute molecular weight. The results stress the need for more work to be undertaken in order to develop predictive models with accuracy sufficient for process design.

Chapter 4: Solubility determination of tolbutamide and butamben and thermodynamic analysis of butamben

4.1 Materials and methods

4.1.1 Materials

Tolbutamide (FI^L) was obtained from Sigma-Aldrich with a purity of 99.7 %. Butamben (FI) was obtained from Changzhou Sunlight Medical Raw with a purity of 99.88 %. Methanol (99.9 %), acetonitrile (99. 9%), ethyl acetate (99.7 %) and toluene (99.9 %) were obtained from Sigma-Aldrich, and 1-propanol (99.7 %), 2-propanol (99.7 %), 1-butanol (99.8 %) were obtained from VWR. All solvents were used as received with no further purification.

4.1.2 PXRD

X-ray powder diffraction (XRPD, Philips PANalytical X'Pert MPD Pro with a PW3064 sample spinner) was used to analyse the sampled excess solid material. Scans in the 2θ range 5-40 ° allowed identification of the polymorph by comparison with the theoretical patterns generated from the structures published in the CSD.

4.1.3 Thermal analysis

The thermal behaviour of solid samples (butamben) was monitored using DSC (PerkinElmer instruments Pyris 1 DSC), at a rate of 10 $K \cdot min^{-1}$, under 50 $mL \cdot min^{-1}$ N_2 purge. Approximately 5 mg of the sample (masses controlled to ± 0.005 mg using Ohaus Analytical Plus electronic balance) was weighed into Al-pans without pinholes (40 μL), which were hermetically sealed *via* a crimper press. The instrument was calibrated with indium (429.75 K, 28.45 $J \cdot g^{-1}$) and lead (600.62 K, 23.01 $J \cdot g^{-1}$).

4.1.4 Preparation of FII of Tolbutamide

For the preparation of FII, FI^L as received from the Sigma was dissolved in toluene and the slurry was agitated for 7 days at ambient temperature. The solvent was then evaporated in a fume hood and the phase identity of the dry powder verified to be pure FII with PXRD and Raman spectroscopy. Butamben as received proved to be Form I by PXRD.

4.1.5 Solubility measurement

Solubility was measured using a gravimetric method. Temperature was controlled using a Grant S26 water bath equipped with a GR150 control unit (specified stability of ±0.005 K) and a Grant C2G cooling unit. A 60-point submersible magnetic stirring plate (2Mag) provided agitation at 600 rpm. The solution was left to be agitated for 24 h to reach equilibrium. In order to make sure that 24 h was enough for reaching equilibrium, concentrations at 24 h and 48 h were measured and the difference in concentrations was less

than 1.5 %. After reaching equilibrium stirring was turned off for approximately 3 h to allow excess solids to settle in vials. Then, from the middle of solution, approximately 5 mL of clear solution were taken in triplicate using pre-heated syringes and filtered through (PTFE or Nylon) filters into pre-weighed glass vials (50 mm × 25 mm). The solution was capped and immediately weighed using a balance. Afterwards, the lids were removed and the solutions placed in a fume hood for approximately two weeks in order to evaporate the solvents. Then when the vials appeared to be visually dry, the vials were placed in an oven at 40 °C for more than 24 h in order to ensure that the samples were solvent free. The weight of the samples was recorded continuously each day until it became constant and solubility was measured. The specified error of the balance used is 0.0001 g. Crystals in the vials were confirmed to be the desirable polymorph by PXRD.

4.2 Solubility of tolbutamide

The solubility of Form II of tolbutamide is reported in Table 4-1.

Table 4-1. Solubility of FII given as g tolbutamide / g solvent together with standard errors

	Methanol	**1-Propanol**	**Ethyl acetate**	**Acetonitrile**	**Toluene**
***T* / °C**	C_{eq} **± s.e. / g g^{-1}**	C_{eq} **± s.e. / g g^{-1}**	C_{eq} **± s.e. / g g^{-1}**	C_{eq} **± s.e. / g g^{-1}**	C_{eq} **± s.e. / g g^{-1}**
5	0.0928 ± 0.00019	0.02999 ± 0.000093	0.0306 ± 0.00044	0.047 ± 0.0028	0.00256 ± 0.000022
10	0.1015 ± 0.00043	0.038 ± 0.0058	0.03407 ± 0.000092	0.058 ± 0.0011	0.0035 ± 0.00013
15	0.1209 ± 0.00099	0.055 ± 0.0010	0.0413 ± 0.00018	0.074 ± 0.0038	0.00437 ± 0.000044
20	0.1481 ± 0.00063	0.067 ± 0.0023	0.051 ± 0.0014	0.0901 ± 0.00094	0.0052 ± 0.00025
25	0.194 ± 0.0015	0.073 ± 0.0022	0.0561 ± 0.00027	0.1003 ± 0.00055	0.00650 ± 0.000046
	Methanol	**1-Propanol**	**Ethyl acetate**	**Acetonitrile**	**Toluene**
30	0.250 ± 0.0015	0.104 ± 0.0085	0.072 ± 0.0028	0.137 ± 0.0027	0.00785 ± 0.000076
35	0.343 ± 0.0020	0.1242 ± 0.00016	0.0936 ± 0.00088	0.1841 ± 0.00012	0.0110 ± 0.00035
40	0.501 ± 0.0083	0.169 ± 0.0046	0.1166 ± 0.00062	0.260 ± 0.0015	0.0148 ± 0.00079

4.3 Solubility of butamben

The solubility of Form I of butamben is reported in Table 4-2.

Table 4-2. Solubility of Form I given as g butamben / g solvent together with standard errors

	Methanol	1-Propanol	2-propanol	1-butanol	Toluene
T / °C	C_{eq} ± s.e. / g g^{-1}	C_{eq} ± s.e. / g g^{-1}	C_{eq} ± s.e. / g g^{-1}	C_{eq} ± s.e. / g g^{-1}	C_{eq} ± s.e. / g g^{-1}
10	0.6761± 0.00011	0.3735± 0.00023	0.3320± 0.00146	0.2831± 0.00038	0.2795± 0.0001
15	1.0018± 0.00211	0.5063± 0.00337	0.4648± 0.00121	0.3833± 0.00844	0.3711± 0.00427
20	1.4931± 0.01833	0.7504± 0.01322	0.7185± 0.0047	0.5804± 0.01592	0.5690± 0.00814
25	2.4193± 0.01484	1.1184± 0.00731	1.0783± 0.0017	0.8425± 0.00304	0.8180± 0.00033

It should be noted that attempts were also made to measure the solubility of butamben (Form I) in ethyl acetate, acetonitrile, acetone and 1,4-dioxane, however in these solvents even at 10 °C the slurry turned a yellow colour after a few hours, showing degradation.

4.4 Thermodynamic analysis of butamben

Figure 4-2 show the DSC diagram obtained in this work. The heat of fusion and melting temperature of Form I were 24.39 kJ/mol and 282.93 K respectively.

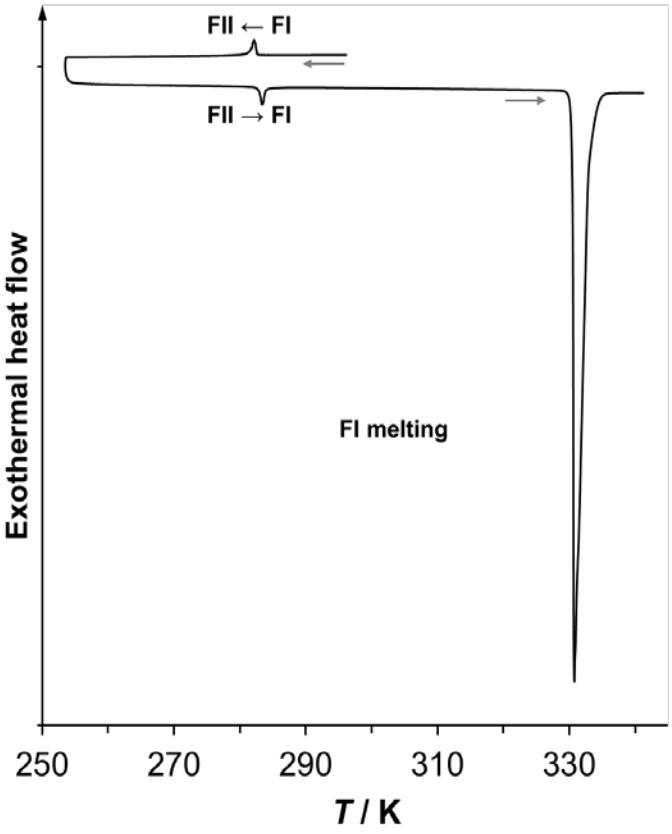

Figure 4-1. DSC diagram of butamben

The solubility values of Form I of butamben are depicted in Figure 4-2.

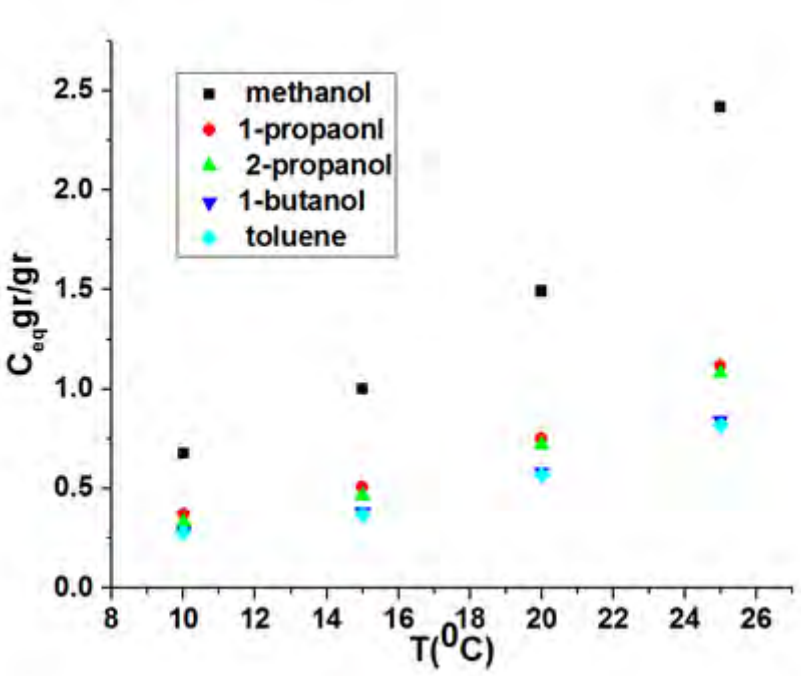

Figure 4-2. Solubility of Form I of butamben in organic solvents as a function of temperature

As shown in Figure 4-2, the solubility was very high in all solvents including both polar and nonpolar solvents, with a maximum value of 2.42 g/g in methanol at 25 °C and the lowest solubility of 0.28 g/g in toluene at 10 °C. With an increasing carbon number in alcohols, the solubility decreased. The solubility order was methanol>1-propanol>2-propanol>1-butanol>toluene. Molecular weight is a property of the solvent that clearly has an influence on the solubility data. As the molecular weight of the solvent increased, the solubility in the solvent decreased. Figure 4-3 shows the relationship between molecular weight and solubility.

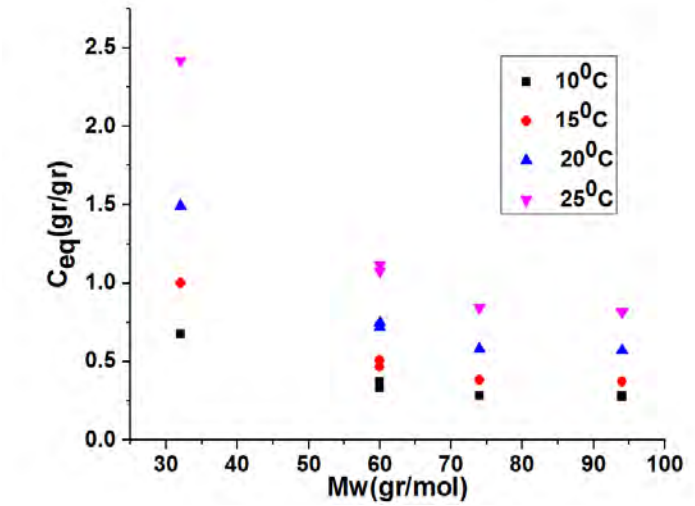

Figure 4-3. Solubility of butamben (Form I) at different temperatures as a function of molecular weight

There is also a clear relationship between the polarity of solvents and solubility. As the polarity of the solvent increases, the solubility also increases.

4.4.1 Prediction of melting temperature

The mole fraction solubility was fitted with the second-order polynomial function:

$$\ln x = \frac{A}{T^2} + \frac{B}{T} + C \qquad (4\text{-}1)$$

In eq.4-1 T is in K and A, B and C are regressed coefficients. Although this equation is very simple, according to the data it is quite an acceptable equation given the small temperature range of this study. The coefficients (A, B and C) for this equation are given in Table 4-3. The Van't Hoff plot is also constructed in Figure 4-5.

Table 4-3. Regression coefficient together with R^2 for equation 4-1 for different solvents

Solvent	**A(K^2)**	**B(K)**	**C**	**R^2**
Methanol	3144152.45	-27495.49	55.5971	0.9997
1-propanol	4581046.78	-36702.07	70.2090	0.9993
2-propanol	3059431.55	-26688.15	53.7199	0.9984
1-butanol	3369370.24	-28420.48	56.0165	0.9968
Toluene	3586991.23	-29694.04	57.9811	0.9963

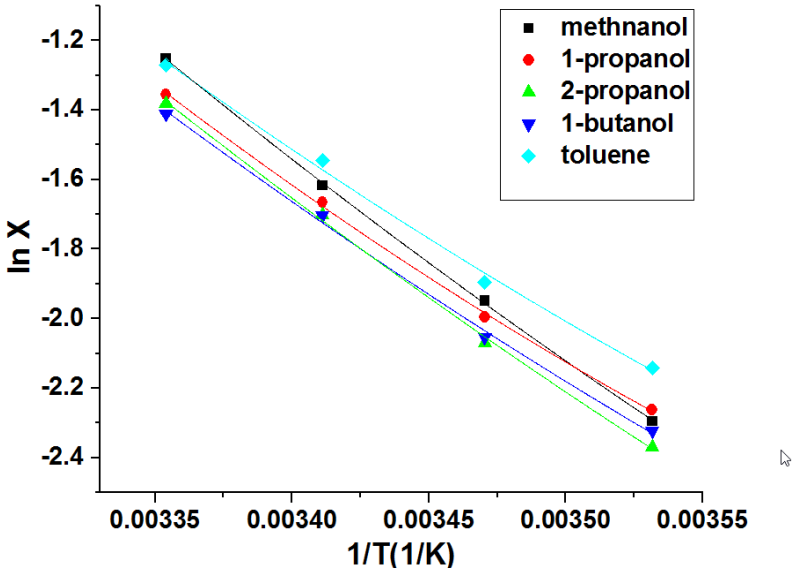

Figure 4-5. Van't Hoff plot of Form I of butamben

At room temperature, the mole fraction solubility was in the order of methanol>toluene>1-propanol>2-propanol>1-butanol. Ideal solubility at room temperature in terms of mole fraction was equal to 0.37, which was very close to the solubility in methanol and toluene (0.28 mole fraction). This behaviour was expected since near the melting point the activity coefficient is close to one, so it can be expected that at high temperatures the solubility is close to ideal solubility. At the lowest investigated temperature (283 K) the ideal solubility was equal to 0.23, which was near the solubility in toluene of 0.10.

If *lnx* in equation 4-1 was set equal to zero, the melting point of the compound could readily be predicted. Based on this, the melting temperatures predicted by extrapolation of the solubility data in methanol, 1-propanol, 2-propanol, 1-butanol and toluene were 42.05 °C, 43.78 °C, 44.36 °C, 45.57 °C and 43.68 °C respectively. As can be seen, the predicted melting temperatures were very close to one other and there was approximately 14 °C difference between the experimental and predicted melting temperatures. This difference shows that it is quite dangerous to extrapolate solubility data outside of the temperature range studied, and even the second-order polynomial failed to predict the melting point with great accuracy.

4.4.2 Calculation of fusion properties

Nordstrom and Rasmuson [72] have evaluated three equations for the effect of the heat capacity term on activity of the solid, neglecting the effect of ΔC_p, ΔC_p equals ΔS^{fusion} at the melting point and finally the correlation of ΔC_p with temperature. The best results in their work were obtained by considering a linear relationship between temperature and ΔC_p, however they found a substantial improvement by equating ΔC_P to $\Delta S^{fusion}(T_m)$ rather than neglecting it entirely. In the present work ΔC_p was set equal to ΔS^{fusion} at a melting point, therefore the activity of a solid can be obtained as follows:

$$\ln a = \frac{\Delta H^{fus}(T_m)}{R T_m} \ln(\frac{T}{T_m}) \qquad (4\text{-}4)$$

In eq.4-4, the melting temperature and heat of fusion can be used to obtain the activity of a solid as a function of temperature. Knowing these parameters, ΔG^{fusion} and ΔH^{fusion} and ΔS^{fusion} can also be calculated as follows:

$$\Delta G^{fus}(T) = \Delta H^{fus}(T) - T\,\Delta S^{fus}(T) = -RT\,\ln a^{solid} \qquad (4\text{-}5)$$

$$\Delta H^{fus}(T) = \Delta H^{fus}(T_m) + \Delta S^{fus}(T_m)(T - T_m) \qquad (4\text{-}6)$$

$$T\,\Delta S^{fus}(T) = \Delta H^{fus}(T_m) - \Delta G^{fus}(T_m) \qquad (4\text{-}7)$$

where $\Delta S^{fusion}(T_m)$ is equal to 73.24 J/mol.

In Figure 4-6, a plot of ΔG^{fusion}, ΔH^{fusion} and ΔS^{fusion} is constructed as a function of temperature.

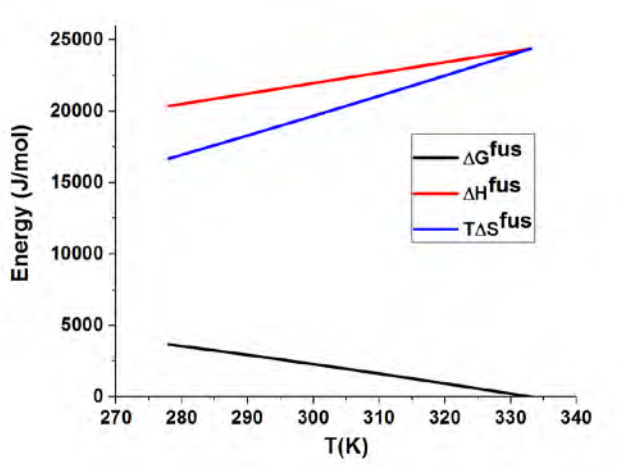

Figure 4-6. Plot of energy as a function of temperature

It can be seen from Figure 4-7 that ΔG^{fusion} decreases as the temperature increases and approaches zero as the Gibbs energy of the two phases are equal in melting temperature. The terms ΔH^{fusion} and $T\Delta S^{fusion}$ also increase with increasing temperature, however the increase of $T\Delta S^{fusion}$ with temperature is greater than the increase of ΔH^{fusion} with temperature.

4.4.3 Calculation of the activity coefficient

Using a combination of equations (4-4) and (1-3), the activity coefficients of Form I of butamben in different organics solvents were calculated as a function of temperature. Figure 4-7 shows the results obtained.

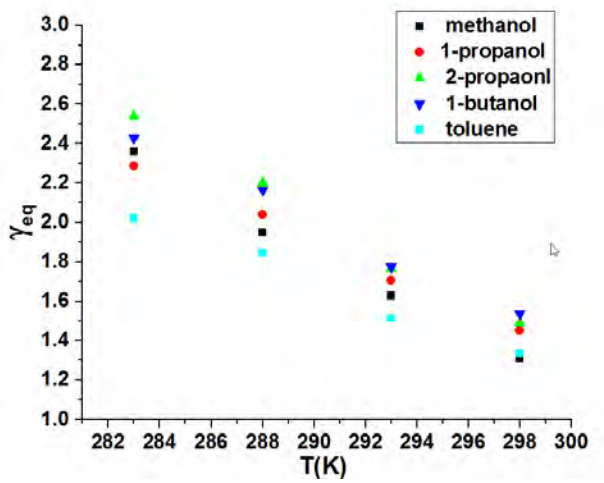

Figure 4-7. Activity coefficient of Form I of butamben as a function of temperature for different solvents

As the graph shows, all systems showed a positive deviation from Raoult's law and as the temperature increased the behaviour of the system moved towards ideality and the activity

coefficient approached one. The data clearly reveal that the solubility of this compound compared to the solubility of other compounds showed that the behaviour was near ideal since the maximum activity coefficient was about 2.6. Since all systems showed a positive deviation from ideality, the summation of solvent-solvent interaction and solute-solute interaction was more than solute-solvent interaction.

4.4.4 Prediction of solubility using one temperature solubility data

Buchowski *et al*. [73] described the behaviour of solid solubility in liquid as the Buchowski equation. This equation gives a good description for many solid-liquid systems using two adjustable parameters, λ and H. Here, instead of fitting these two adjustable parameters to solubility data, a new method was suggested to obtain these parameters utilising data from only one solubility parameter and heat of fusion at melting temperature. The Buchowski equation can be written as:

$$\ln(1+\frac{\lambda(1-x)}{x}) = \lambda H\left(\frac{1}{T}-\frac{1}{T_m}\right) \tag{4-8}$$

Differentiating both the right and left sides yields:

$$\frac{\frac{-\lambda x-\lambda(1-x)}{x^2}}{1+\frac{\lambda(1-x)}{x}}dx = \frac{-\lambda H}{T^2}dT \tag{4-9}$$

and therefore:

$$\frac{d\ln x}{d(\frac{1}{T})} = x^3(-H\lambda)(1+\frac{\lambda(1-x)}{x}) = \frac{-\Delta H^{fus}}{R} \tag{4-10}$$

At melting point $x=1$, $H\lambda$=2933, and from that using data at 20 °C for methanol, 1-propanol, 2-propanol, 1-butanol and toluene λ was equal to 0.7425, 0.6991, 0.6701, 0.6675 and 0.8153 respectively. The averages ARD of solubility prediction using this method were 0.13, 0.09, 0.1, 0.09 and 0.09 for methanol, 1-propanol, 2-propanol, 1-butanol and toluene respectively. Therefore the result of prediction is quite acceptable. The plot of predicted *versus* experimental solubility in mole fraction is constructed in Figure 4-8 for methanol.

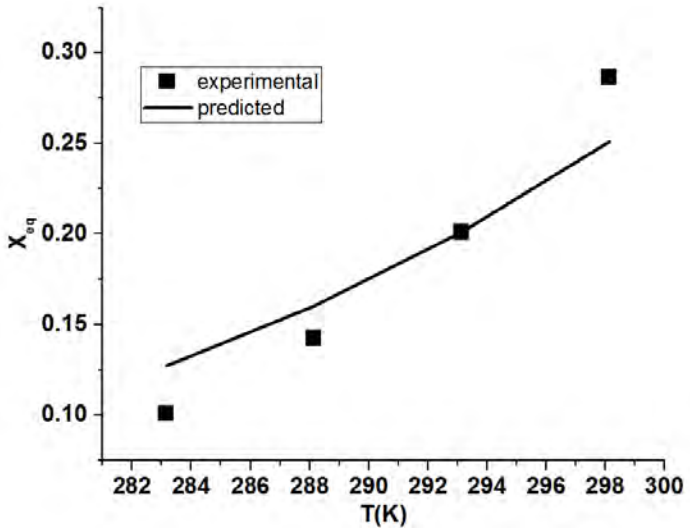

Figure 4-8. Prediction of solubility of Form I of butamben in methanol using the Buchowski equation

Chapter 5: Conclusions

5.1 **Conclusions**

Solubility and the activity coefficient are two thermodynamic properties that strongly affect the crystallisation outcome such as crystal shape and size. The activity coefficient and solubility are strongly related since for the same API the change in solubility directly resulted in a change in the activity coefficient. Therefore the aim of this work was to investigate these two thermodynamic parameters in detail. This project was divided into three sections: the activity coefficient investigation using VLE data, solubility prediction and the experimental investigation of solubility. However these sections are related since knowledge of solubility is crucial to understanding how the solution behaves far from ideality (magnitude of activity coefficient). The conclusions for each section are given below.

Using VLE data for 30 binary mixtures, this project investigated the influence of temperature and composition on the activity coefficient. The effect of temperature on the activity coefficient was found to be less than the corresponding effect of composition. The results showed that the maximum effect of temperature on the activity coefficient could be seen in a dilute range. Furthermore, an analysis was performed to investigate errors stemming from neglecting temperature and composition on the activity coefficient for the calculation of the driving force for nucleation. It was found that in general, neglecting the composition dependence of the activity coefficient produced more errors than neglecting the temperature dependence of the activity coefficient. Therefore, in order to estimate the driving force for crystallisation it would be more accurate to neglect just the temperature effect on the activity coefficient rather than completely neglect the effects of both temperature and composition on the activity coefficient.

The solubility of five APIs was modelled using the temperature-independent NRTL-SAC model and the temperature dependent NRTL-SAC model. In addition, the solubility of three APIs was modelled using the Pharma UNIFAC model. It was found that introducing a temperature-dependent binary interaction parameter to the temperature-independent NRTL-SAC model could, in general, improve the performance of this model for modelling vapour-liquid equilibria and solid-liquid equilibria. The results also showed that if the NRTL-SAC was seen as a predictive tool, the NRTL-SAC model showed a better performance than the Pharma UNIFAC model.

The solubilities of two APIs, tolbutamide (Form II) and butamben (Form I), were experimentally measured. It was found that for the entire range of solvents investigated, the

solubility of both APIs increased with increasing temperature. The thermodynamics of Form I of butamben in solution was also investigated. A relationship between the molecular weight of the solvent and the polarity of the solvent and solubility of Form I of butamben was found. In addition, the solubility of butamben (Form I) was predicted using just one solubility data point by employing the Buchowski equation with quite acceptable accuracy.

References

1. Valder, C.; Merrifield, D., Pharmaceutical technology. *SmithKline Beecham R&D News* **1996,** *32* (1).

2. Mullin, J. W., *Crystallisation*. Butterworths London: 1972.

3. Abrams, D. S.; Prausnitz, J. M., Statistical thermodynamics of liquid mixtures: a new expression for the excess Gibbs energy of partly or completely miscible systems. In *AIChE Journal*, 1975; Vol. 21, pp 116-128.

4. Fredenslund, A.; Jones, R. L.; Prausnitz, J. M., Group-contribution estimation of activity coefficients in nonideal liquid mixtures. *AIChE Journal* **1975,** *21* (6), 1086-1099.

5. Mullins, E.; Liu, Y.; Ghaderi, A.; Fast, S. D., Sigma profile database for predicting solid solubility in pure and mixed solvent mixtures for organic pharmacological compounds with COSMO-based thermodynamic methods. *Industrial & Engineering Chemistry Research* **2008,** *47* (5), 1707-1725.

6. Ruether, F.; Sadowski, G., Modeling the solubility of pharmaceuticals in pure solvents and solvent mixtures for drug process design. *Journal of pharmaceutical sciences* **2009,** *98* (11), 4205-4215.

7. Chen, C.-C.; Song, Y., Solubility modeling with a nonrandom two-liquid segment activity coefficient model. *Industrial & engineering chemistry research* **2004,** *43* (26), 8354-8362.

8. Mota, F. L.; Carneiro, A. P.; Queimada, A. J.; Pinho, S. P.; Macedo, E. A., Temperature and solvent effects in the solubility of some pharmaceutical compounds: Measurements and modeling. *European Journal of Pharmaceutical Sciences* **2009,** *37* (3), 499-507.

9. Diedrichs, A.; Gmehling, J. r., Solubility calculation of active pharmaceutical ingredients in alkanes, alcohols, water and their mixtures using various activity coefficient models. *Industrial & Engineering Chemistry Research* **2010,** *50* (3), 1757-1769.

10. Tung, H. H.; Tabora, J.; Variankaval, N.; Bakken, D.; Chen, C. C., Prediction of pharmaceutical solubility Via NRTL-SAC and COSMO-SAC. *Journal of Pharmaceutical Sciences* **2008,** *97* (5), 1813-1820.

11. Sheikholeslamzadeh, E.; Rohani, S., Solubility prediction of pharmaceutical and chemical compounds in pure and mixed solvents using predictive models. *Industrial & Engineering Chemistry Research* **2011,** *51* (1), 464-473.

12. Na, H.-S.; Arnold, S.; Myerson, A. S., Water activity in supersaturated aqueous solutions of organic solutes. *Journal of crystal growth* **1995,** *149* (3), 229-235.

13. Watterson, S.; Hudson, S.; Svärd, M.; Rasmuson, Å. C., Thermodynamics of fenofibrate and solubility in pure organic solvents. *Fluid Phase Equilibria* **2014,** *367*, 143-150.

14. Thirunahari, S.; Aitipamula, S.; Chow, P. S.; Tan, R. B., Conformational polymorphism of tolbutamide: A structural, spectroscopic, and thermodynamic

characterization of Burger's forms I–IV. *Journal of pharmaceutical sciences* **2010,** *99* (7), 2975-2990.

15. Schmidt, A., Structural characteristics and crystal polymorphism of three local anaesthetic bases: crystal polymorphism of local anaesthetic drugs: part VII. *International journal of pharmaceutics* **2005,** *298* (1), 186-197.

16. J. GMEHLING, U. O., W. ARLT, P. GRENZHEUSER, U. WEIDLICH, B. KOLBE, J. RAREY, Vapor-Liquid Equilibrium Data Collection. *DECHEMA* **1991 - 2014,** *I*.

17. Van Ness, H. C.; Byer, S. M.; Gibbs, R. E., Vapor-Liquid equilibrium: Part I. An appraisal of data reduction methods. *AIChE Journal* **1973,** *19* (2), 238-244.

18. D Avilla S.G, C. J. O. B., *private communication*

19. Mertl, I., Liquid-vapour equilibrium. IL. Phase equilibria in the ternary system ethyl acetate-ethanol-water. *Collection of czechoslovak chemical communications* **1972,** *37* (2), 366-374.

20. Udovenko, V.; Mazanko, T.; Plyngeu, V. Y., Liquid-vapor equilibrium in normal propyl alcohol-water and normal propyl alcohol benzene systems. MEZHDUNARODNAYA KNIGA 39 DIMITROVA UL., 113095 MOSCOW, RUSSIA: 1972; Vol. 46, pp 218-&.

21. Vrevsky, M., Composition and vapor tension of solutions. *Zh. Russ. Fiz.-Khim. Obshch* **1910,** *42*, 1-35.

22. Schreiber, E.; Schuettau, E.; Rant, D.; Schuberth, H., Extent to which a metal chloride can influence the behavior of isothermal phase equilibrium in n-propanol-water and nbutanol-water systems. *Z. Phys. Chem.(Leipzig)* **1971,** *247*, 23-40.

23. SADA, E.; MORISUE, T., Isothermal vapor-liquid equilibrium data of isopropanol-water system. *Journal of Chemical Engineering of Japan* **1975,** *8* (3), 191-195.

24. von N, I.; Dändliker, G.; Trümpler, G., Ueber das Verdampfungsgleichgewicht des Systems Wasser—Pyridin. *Chemical Engineering Science* **1956,** *5* (4), 193-197.

25. Andon, R.; Cox, J.; Herington, E., Phase relationships in the pyridine series. Part 6. The thermodynamic properties of mixtures of pyridine, and of three of its homologues, with water. *Trans. Faraday Soc.* **1957,** *53*, 410-426.

26. Nagata, I.; Yamada, T.; Nakagawa, S., Excess Gibbs free energies and heats of mixing for binary systems ethyl acetate with methanol, ethanol, 1-propanol, and 2-propanol. *Journal of Chemical and Engineering Data* **1975,** *20* (3), 271-275.

27. Freshwater, D. C.; Pike, K. A., Vapor-liquid equilibrium data for systems of acetone-methanol-isopropanol. *Journal of Chemical and Engineering Data* **1967,** *12* (2), 179-183.

28. Marinichev, A.; Susarev, M., Liquid-vapor equilibrium in the system methanol-cyclohexane at 35, 45, and 55 0C and 760 mm Hg. *Zh. Prikl. Khim.(Leningrad)* **1965,** *38*, 1619-1621.

29. Bekarek, V., Liquid-vapour equilibrium. XL. Liquid-vapour equilibrium in the systems SO 2-CH 3 COOH 3-CH 3 OH and SO 2-CH 3 COH 3-CH 3 OH. *Collection of Czechoslovak Chemical Communications* **1968,** *33* (8), 2608-2619.

30. Bredig, G.; Bayer, R., The vapor pressure of the system methanol-water. *Z. physik. Chem* **1927,** *130*, 1-14.

31. Gordon, A.; Hines, W., LIQUID-VAPOUR EQUILIBRIUM FOR THE SYSTEM ETHANOL-ACETONE. *Canadian Journal of Research* **1946,** *24* (5), 254-262.

32. Scatchard, G.; Raymond, C., Vapor—liquid equilibrium. II. Chloroform—ethanol mixtures at 35, 45 and 55°. *Journal of the American Chemical Society* **1938,** *60* (6), 1278-1287.

33. p., E., *diplomarbeit dourtmound* **1975**.

34. Murti, P.; Van Winkle, M., Vapor-liquid equilibria for binary systems of methanol, ethyl alcohol, 1-propanol, and 2-propanol with ethyl acetate and 1-propanol-water. *Industrial & Engineering Chemistry Chemical and Engineering Data Series* **1958,** *3* (1), 72-81.

35. Scatchard, G.; Satkiewicz, F. G., Vapor-liquid equilibrium. XII. The system ethanol-cyclohexane from 5 to 65°. *Journal of the American Chemical Society* **1964,** *86* (2), 130-133.

36. Nagai, J.; Ishii, N., Volatility of Fuels Containing Ethyl Alcohol. I. Partial Pressures of Ethyl Alcohol and Ethyl Ether in Their Mixtures and Calculation of Heat of Mixture. *J. Soc. Chem. Ind. Japan* **1935,** *38*, 8-12.

37. Kretschmer, C. B.; Wiebe, R., Liquid-Vapor Equilibrium of Ethanol--Toluene Solutions. *Journal of the American Chemical Society* **1949,** *71* (5), 1793-1797.

38. Wright, W. A., A Method for a More Complete Examination of Binary Liquid Mixtures. *The Journal of Physical Chemistry* **1933,** *37* (2), 233-243.

39. Smith, V. C.; Robinson Jr, R. L., Vapor-liquid equilibriums at 25. deg. in the binary mixtures formed by hexane, benzene, and ethanol. *Journal of Chemical and Engineering Data* **1970,** *15* (3), 391-395.

40. Udovenko, V.; Fatkulina, L., Vapor pressure of three-component systems. I. The system ethyl alcohol-1, 2-dichloroethane-benzene. *Zh. Fiz. Khim* **1952,** *26*, 719-730.

41. Yuan, K. S.; Ho, J. C.; Koshpande, A.; Lu, B. C.-Y., Vapor-Liquid Equilibria. *Journal of Chemical and Engineering Data* **1963,** *8* (4), 549-559.

42. Smyth, C.; Engel, E., Molecular orientation and the partial vapor pressures of binary mixtures. I. Systems composed of normal liquids. *Journal of the American Chemical Society* **1929,** *51* (9), 2646-2660.

43. Linek, J.; Procházka, K.; Wichterle, I., Liquid-vapour equilibrium. LIV. The systems ethyl acetate-benzene, ethyl acetate-toluene and ethyl acetate-ethylbenzene. *Collection of Czechoslovak Chemical Communications* **1972,** *37* (9), 3010-3014.

44. Markuzin, N.; Pavlova, L., Liquid-vapor equilibriums in an acetic acid-heptane-toluene system. I. Experimental data based on equilibrium in binary systems and a calculation of the dimerization constant for acetic acid in the vapor. *Zh Prikl Khim (Sankt-Petersburg, Russian Federation)* **1971,** *44*, 311-315.

45. Linek, J.; Wichterle, I.; Polednova, J., Liquid-vapour equilibrium. LIII. The systems benzene-diisopropyl ether, diisopropyl ether-toluene, diisopropyl ether-ethylbenzene, benzene-dipropyl ether, dipropyl ether-toluene and dipropyl ether-ethylbenzene. *Collection of Czechoslovak Chemical Communications* **1972,** *37* (9), 2820-2829.

46. Boublik, T., An estimate of limiting values of relative volatility with help of the theorem of corresponding states. II. Binary systems of tetrachloromethane, benzene, and cyclohexane. *Collection of Czechoslovak Chemical Communications* **1963,** *28* (7), 1771-1779.

47. Fowler, R.; Lim, S., Azeotropism in binary solutions: Carbon tetrachloride-benzene system. *Journal of Applied Chemistry* **1956,** *6* (2), 74-78.

48. Scatchard, G.; Wood, S.; Mochel, J., Vapor-Liquid Equilibrium. V. Carbon Tetrachloride-Benzene Mixtures1. *Journal of the American Chemical Society* **1940,** *62* (4), 712-716.

49. Gaw, W.; Swinton, F., Thermodynamic properties of binary systems containing hexafluorobenzene. Part 3.—Excess Gibbs free energy of the system hexafluorobenzene+ cyclohexane. *Transactions of the Faraday Society* **1968,** *64*, 637-647.

50. Gaw, W.; Swinton, F., Thermodynamic properties of binary systems containing hexafluorobenzene. Part 4.—Excess Gibbs free energies of the three systems hexafluorobenzene+ benzene, touene, and p-xylene. *Transactions of the Faraday Society* **1968,** *64*, 2023-2034.

51. Wang, J.; Boublikova, L.; Lu, B. Y., Vapour-liquid equilibria of the carbon tetrachloride-toluene system. *Journal of Applied Chemistry* **1970,** *20* (6), 172-174.

52. Werner, G.; Schuberth, H., Das Phasengleichgewicht flüssig-flüssig des Systems Benzol/n-Heptan/Acetonitril sowie die Phasengleichgewichte dampfförmig-flüssig der entsprechenden binären Systeme bei 20, 0° C. *Journal für Praktische Chemie* **1966,** *31* (5-6), 225-239.

53. Kudryavtseva, L.; Viit, K.; Eizen, O., Eesti NSV Tead. *Akad. Toim. Keem. Geol* **1971,** *20*, 292-299.

54. Bayles, J. W.; Letcher, T. M., Thermodynamics of some binary liquid mixtures containing aliphatic amines. *Journal of Chemical & Engineering Data* **1971,** *16* (3), 266-271.

55. Geiseler, G.; Koehler, H., Thermodynamisches Verhalten der Mischsysteme Methyläthylketoxim/n-Heptan, Diäthylketon/n-Heptan und Methyläthylketoxim/Diäthylketon. *Berichte der Bunsengesellschaft für physikalische Chemie* **1968,** *72* (6), 697-706.

56. Bennett, G. W., A laboratory experiment on the boiling-point curves of non-azeotropic binary mixtures. *Journal of Chemical Education* **1929,** *6* (9), 1544.

57. Rius, A.; Otero, J.; Macarron, A., Equilibres liquide—vapeur de mélanges binaires donnant une réaction chimique: systèmes méthanol—acide acétique; éthanol—acide acétique; n-propanol—acide acétique; n-butanol—acide acétique. *Chemical Engineering Science* **1959,** *10* (1), 105-111.

58. Nagata, I.; Tamura, K., Excess molar enthalpies of {methanol or ethanol+(2-butanone+ benzene)} at 298.15 K. *The Journal of Chemical Thermodynamics* **1990,** *22* (3), 279-283.

59. Nielsen, R. L.; Weber, J. H., Vapor-Liquid Equilibria at Subatmospheric Pressures. Binary and Ternary Systems Containing Ethyl Alcohol, Benzene, and n-Heptane. *Journal of Chemical and Engineering Data* **1959,** *4* (2), 145-151.

60. Jasra, R.; Nageshkumar, V.; Ramachandran, S.; Bhat, S., EXCESS MOLAR VOLUMES OF BINARY-MIXTURES OF ALKYL SUBSTITUTED BENZENE (S) AND OCTANE (S) AT 298.15 K. *INDIAN JOURNAL OF TECHNOLOGY* **1988,** *26* (6), 297-300.

61. Carr, A.; Kropholler, H., Vapor liquid equilibria at atmospheric pressure. binary systems of ethyl acetate-benzene, ethyl acetate-toluene, and ethyl acetate-p-xylene. *Journal of Chemical and Engineering Data* **1962,** *7* (1), 26-28.

62. Tasić, A.; Djordjević, B.; Grozdanić, D.; Afgan, N.; Malić, D., Vapour—liquid equilibria of the systems acetone—benzene, benzene—cyclohexane and acetone—cyclohexane at 25° C. *Chemical Engineering Science* **1978,** *33* (2), 189-197.

63. Nordström, F. L.; Rasmuson, Å. C., Solubility and Melting Properties of Salicylamide. *J. Chem. Eng. Data* **2006,** *51* (5), 1775-1777.

64. Yang, H.; Thati, J.; Rasmuson, Å. C., Thermodynamics of molecular solids in organic solvents. *Journal of Chemical Thermodynamics* **2012,** *48*, 150-159.

65. Kuhs, M.; Svärd, M.; Rasmuson, Å. C., Thermodynamics of fenoxycarb in solution. *J. Chem. Thermodyn.* **2013,** *66*, 50-58.

66. Sun, X.-H.; Liu, Y.-F.; Tan, Z.-C.; Jia, Y.-Q.; Yang, J.-W.; Wang, M.-H., Heat capacity and enthalpy of fusion of fenoxycarb. *Chinese Journal of Chemistry* **2005,** *23* (5), 501-505.

67. Mealey, D.; Svärd, M.; Rasmuson, Å. C., Thermodynamics of risperidone and solubility in pure organic solvents. *Fluid Phase Equilib.* **2014,** *375*, 73-79.

68. Gmehling, J.; Onken, U.; Arlt, W.; Grenzheuser, P.; Weidlich, U.; Kolbe, B.; Rarey, J., *Vapor-Liquid Equilibrium Data Collection*. Frankfurt, 1991 - 2014.

69. Kuhs, M.; Svärd, M.; Rasmuson, Å. C., Thermodynamics of fenoxycarb in solution. *The Journal of Chemical Thermodynamics* **2013,** *66*, 50-58.

70. Yang, H.; Rasmuson, Å. C., Solubility of butyl paraben in methanol, ethanol, propanol, ethyl acetate, acetone, and acetonitrile. *Journal of Chemical & Engineering Data* **2010,** *55* (11), 5091-5093.

71. Nordström, F. L.; Rasmuson, Å. C., Solubility and melting properties of salicylamide. *Journal of Chemical & Engineering Data* **2006,** *51* (5), 1775-1777.

72. Nordström, F. L.; Rasmuson, Å. C., Prediction of solubility curves and melting properties of organic and pharmaceutical compounds. *european journal of pharmaceutical sciences* **2009,** *36* (2), 330-344.

73. Buchowski, H.; Ksiazczak, A.; Pietrzyk, S., Solvent activity along a saturation line and solubility of hydrogen-bonding solids. *The Journal of Physical Chemistry* **1980,** *84* (9), 975-979.